

Journal Pre-proofs

Discovery of new ATP-competitive inhibitors of human DNA topoisomerase II α through screening of bacterial topoisomerase inhibitors

Žiga Skok, Martina Durcik, Darja Gramec Skledar, Michaela Barančoková, Lucija Peterlin Mašič, Tihomir Tomašič, Anamarija Zega, Danijel Kikelj, Nace Zidar, Janez Ilaš

PII: S0045-2068(20)31346-8
DOI: <https://doi.org/10.1016/j.bioorg.2020.104049>
Reference: YBIOO 104049

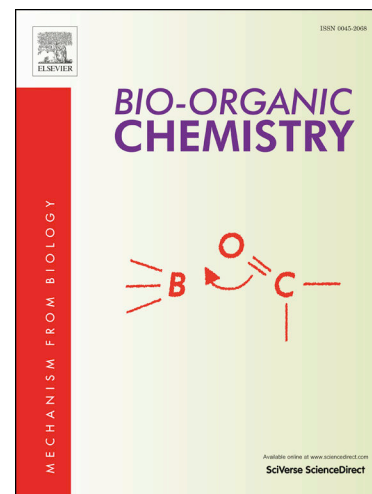
To appear in: *Bioorganic Chemistry*

Received Date: 12 April 2020
Revised Date: 19 June 2020
Accepted Date: 25 June 2020

Please cite this article as: Z. Skok, M. Durcik, D. Gramec Skledar, M. Barančoková, L. Peterlin Mašič, T. Tomašič, A. Zega, D. Kikelj, N. Zidar, J. Ilaš, Discovery of new ATP-competitive inhibitors of human DNA topoisomerase II α through screening of bacterial topoisomerase inhibitors, *Bioorganic Chemistry* (2020), doi: <https://doi.org/10.1016/j.bioorg.2020.104049>

This is a PDF file of an article that has undergone enhancements after acceptance, such as the addition of a cover page and metadata, and formatting for readability, but it is not yet the definitive version of record. This version will undergo additional copyediting, typesetting and review before it is published in its final form, but we are providing this version to give early visibility of the article. Please note that, during the production process, errors may be discovered which could affect the content, and all legal disclaimers that apply to the journal pertain.

© 2020 Elsevier Inc. All rights reserved.



Discovery of new ATP-competitive inhibitors of human DNA topoisomerase II α through screening of bacterial topoisomerase inhibitors

Žiga Skok, Martina Durcik, Darja Gramec Skledar, Michaela Barančoková, Lucija Peterlin Mašič, Tihomir Tomašič, Anamarija Zega, Danijel Kikelj, Nace Zidar* and Janez Ilaš*

University of Ljubljana, Faculty of Pharmacy, Aškerčeva cesta 7, 1000 Ljubljana, Slovenia

*Corresponding author: Janez Ilaš

Aškerčeva cesta 7

1000 Ljubljana, Slovenia

Tel: +386-1-4769576

E-mail: janez.ilas@ffa.uni-lj.si

*Corresponding author: Nace Zidar

Aškerčeva cesta 7

1000 Ljubljana, Slovenia

Tel: +386-1-4769564

E-mail: nace.zidar@ffa.uni-lj.si

ABSTRACT

Human DNA topoisomerase II is one of the major targets in anticancer therapy, however ATP-competitive inhibitors of this target have not yet reached their full potential. ATPase domain of human DNA topoisomerase II belongs to the GHKL ATPase superfamily and shares a very high 3D structural similarity with other superfamily members, including bacterial topoisomerases. In this work we report the discovery of a new chemotype of ATP-competitive inhibitors of human DNA topoisomerase II α that were discovered through screening of in-house library of ATP-competitive inhibitors of bacterial DNA gyrase and topoisomerase IV. Systematic screening of this library provided us with 20 hit compounds. 1,2,4-Substituted *N*-phenylpyrrolamides were selected for a further exploration which resulted in 13 new analogues, including **52** with potent activity in relaxation assay ($IC_{50} = 3.2 \mu\text{M}$) and ATPase assay ($IC_{50} = 0.43 \mu\text{M}$). Cytotoxic activity of all hits was determined in MCF-7 cancer cell line and the most potent compounds, **16** and **20**, showed an IC_{50} value of 8.7 and 8.2 μM , respectively.

KEYWORDS: anticancer drug, ATP-competitive inhibitor, biological screening, DNA topoisomerase II, *N*-phenylpyrrolamide

ABBREVIATIONS

AMP-PNP, adenylyl-imidodiphosphate; DIAD; diisopropyl azodicarboxylate; DMAP, 4-dimethylaminopyridine; GHKL, gyrase, Hsp90, histidine kinase and MutL; GyrA, DNA gyrase subunit A; GyrB, DNA gyrase subunit B; topo II, human DNA topoisomerase II.

1. INTRODUCTION

Topoisomerases are a family of enzymes with ability to change the topology of DNA molecule. Based on their structure and mechanism of action, topoisomerases can be divided into two types. Type I topoisomerases are monomeric enzymes that catalyse single-strand breaks in DNA double helix, while multimeric type II topoisomerases catalyse double-strand breaks. Based on structural and functional distinctions, both types of topoisomerases are further divided into two subfamilies: IA and IB, and IIA and IIB. Topoisomerases have important roles in processes such as replication and transcription and are essential for cell survival; hence their inhibition leads to cell death. Bacterial type IIA topoisomerases (DNA gyrase and DNA topoisomerase IV) are well known targets of antibacterial drugs, while human DNA topoisomerase IIA (topo II) is targeted by anticancer agents such as etoposide, doxorubicin, daunorubicin and mitoxantrone [1,2].

Prokaryotic and eukaryotic type IIA topoisomerases share many structural and functional similarities. They all require Mg(II) ions as cofactors and the energy from ATP hydrolysis to perform their function. Prokaryotic topoisomerase IIA enzymes have heterotetrameric structure, while eukaryotic enzymes are homodimeric. All type IIA topoisomerases have a three-domain structure, which was determined based on their homology with *Escherichia coli* DNA gyrase. Subunit B of *E. coli* DNA gyrase (GyrB) is homologous to the N-terminal part of topo II, subunit A of *E. coli* DNA gyrase (GyrA) is homologous to the central domain of topo II, and the C-terminal tail of both enzymes is responsible for their nuclear localization and for their interactions with other proteins. The ATP binding sites lie within the N-terminal domains of type IIA topoisomerases. The ATPase domain belongs to the GHKL superfamily (gyrase, Hsp90, histidine kinase and MutL) whose members contain a unique Bergerat fold. Despite low sequence homology between GHKL proteins, the 3D structures of their ATP binding domains are almost superimposable [2–4].

There are many known crystal structures of *E. coli* GyrB with bound inhibitors (for example PDB: 4ZVI [5], 1KZN [6], 6F86 [7], 6F8J [7], 6F94 [7], 6F96 [7], 5MMN [8], 5MMO [8], 5MMP [8], 4DUH [9], 3G7E [10]) and recently a full structure of *E. coli* gyrase was resolved with cryo-EM (PDB: 6RKU [11]). On the other hand, the crystal structure of ATPase domain of topo II with bound inhibitor is not yet known, however, crystal structures with ATP analogues are available (PDB: 1ZXN [12], 1ZXM [12]). Figure 1 shows the comparison of the binding poses of ATP analogues adenosine diphosphate (ADP) and adenylyl-imidodiphosphate

(AMP-PNP) in the ATP binding site of *E. coli* GyrB and topo II. The main interactions in both enzymes are hydrogen bonds of the adenine ring with Asp73 of *E. coli* GyrB or Asn120 of topo II and interactions of the phosphate moiety with Mg(II) ions and multiple amino acid residues in the phosphate binding pocket.

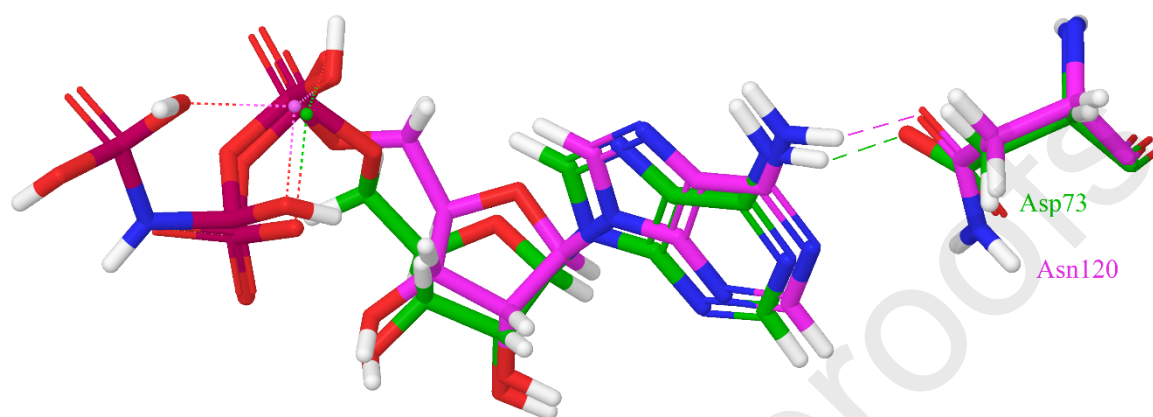


Figure 1: Comparison of binding conformation of ADP in the ATP binding site of *E. coli* DNA gyrase (PDB: 4PRV, carbon atoms coloured in green) and binding pose of AMP-PNP (a non-hydrolysable analogue of ATP) in the ATP binding site of topo II α (PDB: 1ZXM, carbon atoms coloured in purple) after binding site alignment. Key interactions of both ligands with Asp73/Asn120 and Mg(II) ions are shown as dashed lines. Figure was generated using Schrödinger Release 2016-2 (Binding site alignment, Schrödinger, LLC, New York, NY, USA, 2016).

Topo II exists in two isoforms, α and β . The expression of topo II α is dependent on the cell cycle step and is distinctive for the proliferating cells, and essential for their survival [13]. The main function of the α isoform is to release the DNA topology strains that are created during DNA replication and mitosis [14]. Topo II β is expressed in all post-mitotic cells independent of the cell cycle, and while it shows similar function to α isoform *in vitro*, its *in vivo* role is poorly understood. Topo II β seems not to be essential in the proliferating cells, however, the current findings support its important function in local regulation of chromatin architecture. In mice, the genetic deletion of topo II β resulted in perinatal defects and death [14,15].

Topo II inhibitors can be divided into two large groups, topo II poisons and catalytic inhibitors. Clinically successful topo II inhibitors belong in the first group, which act through stabilising the covalent enzyme–DNA complex, either through slowing down the religation step

or speeding up the complex formation. As a consequence, increased levels of damaged DNA are present in the cells, which – if not repaired – leads to cell death. Catalytic inhibitors act through various mechanisms, such as blocking the ATP binding site, preventing the binding of topo II on DNA, or inhibiting the formation of covalent cleavable complex. The only approved drug from this group of inhibitors is dexrazoxane, which inhibits topo II cleavage reaction, but is only used in the clinic in combination with doxorubicin to antagonise its cardiotoxicity [1,16].

Topo II poisons used in the clinic were discovered in the 1960s and 1970s and have remained a clinically important class of anticancer drugs. There are some issues connected to the use of topo II poisons in therapy, such as toxicity (eg. secondary leukaemia, cardiotoxicity and myelosuppression) and development of resistance [1,17]. Because of these liabilities, catalytic inhibitors of topo II represent an interesting alternative to topo II poisons with potentially lower toxicity. Among catalytic inhibitors, ATP-competitive inhibitors show good promise, especially considering the recent clinical success of some other ATP-competitive inhibitors, such as kinase inhibitors [18,19]. Additionally, the unique GHKL ATP binding site architecture makes the non-specific binding of topo II inhibitors to non-GHKL kinases unlikely [4,20]. Several ATP-competitive inhibitors of topo II have been reported, most of which are purine analogues, including the most promising inhibitor described so far, QAP1, which was developed by Novartis. The inhibitory activity of QAP1 on topo II was determined with ATPase assay ($IC_{50} = 128 \text{ nM}$) and its cytotoxicity was evaluated with MTT assay on SK-BR-3 and MCF-7 cancer cell lines (IC_{50} values $10 \text{ }\mu\text{M}$ and $32 \text{ }\mu\text{M}$ respectively) [21,22]. Other structural types of topo II ATP-competitive inhibitors include thiosemicarbazones [23], N-fused imidazoles [24], urothilins [25], xanthenes [26] and triazinones [27]. Novobiocin, a known ATP-competitive inhibitor of bacterial topoisomerases, also shows very weak inhibitory activity on topo II ($IC_{50} = 650 \text{ }\mu\text{M}$), however, it is highly selective for bacterial topoisomerases (*E. coli* DNA gyrase $IC_{50} = 98 \text{ nM}$) [28].

2. RESULTS AND DISCUSSION

2.1. Screening of library of bacterial topoisomerase inhibitors

We have recently discovered several new classes of ATP-competitive inhibitors of bacterial topoisomerases [5,29–34]. Our in-house library is structurally based on natural products oroidin and kibdelomycin. The latter shows antibacterial activity and binds to the ATP binding site of bacterial topoisomerases [35,36]. Both natural compounds share a pyrrolamide moiety which seems to be important for the binding in the ATP binding site (Figure 2). Indeed,

the crystal structure of kibelomycin in ATP binding site of *S. aureus* DNA gyrase shows that this part of the molecule forms a hydrogen bond with Asp81 (Asp73 according to *E. coli* DNA gyrase numbering) [37].

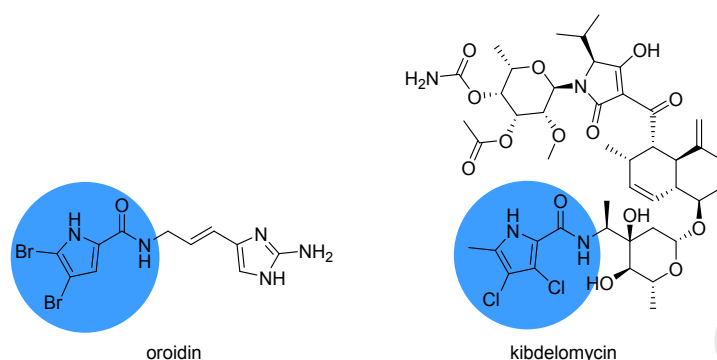


Figure 2: Structures of natural compounds oroidin and kibelomycin with highlighted pyrrolamide moieties.

Approximately 1000 ATP-competitive pyrrolamide-type inhibitors of DNA gyrase and topoisomerase IV were synthesized in the previous work of our research group. From this library, 112 structurally diverse representative compounds were selected and screened against human topo II α using relaxation assay. The majority of molecules contained a pyrrole moiety or its bioisostere that can – similarly as in oroidin and kibelomycin – bind to the adenine binding pocket and form a hydrogen bond with Asp73. This binding mode was confirmed with the obtained crystal structures of two inhibitors from this library in the ATP binding site of *E. coli* DNA gyrase [31,34]. Based on the central scaffold, the selected compounds can be divided into derivatives of the 4,5,6,7-tetrahydrobenzothiazole (25 compounds), benzene (24 compounds), piperidine or piperazine (14 compounds), benzothiazole (12 compounds), thiazole (6 compounds), benzoxazine (6 compounds), pyrrole (5 compounds), and miscellaneous compounds (20 compounds). Structures of all 112 screened compounds are shown in Table S1 of the Supporting information. Compounds were screened at 100 μ M and 10 μ M concentrations. For compounds with residual activities lower than 60% at 100 μ M, IC₅₀ values were determined using seven concentration points. This initial screening provided nine hit compounds with IC₅₀ values lower or equal to 120 μ M, at hit rate of approximately 8%. Structures of hit compounds **1-9** and their activities are presented in Figure 3.

Out of nine hits, five had a benzene central scaffold, two had a benzothiazole scaffold, one had a thiazole, and one had an indole central scaffold. The most potent compound was benzene derivative **6** with an IC₅₀ of 7.2 μ M. A preliminary SAR was estimated for this series.

The substituents on the pyrrole ring have a major effect on the activity of compounds. In all structural types, compounds with 3,4-dichloro-5-methylpyrrole showed much stronger activities than compounds with 4,5-dibromopyrrole. Compounds with other substituents on the pyrrole ring (e.g. monochloro, monobromo or dichloro) were inactive. For benzene-type compounds, it seems that 1,2,4 substitution pattern on the benzene ring is necessary for potent activity, with isopropoxy group (**6**; $IC_{50} = 7.2 \mu M$) being preferred to methoxy group (**3**; $IC_{50} = 29 \mu M$) in position 2. All nine hits had an acidic group on the right-hand side of the molecules – eight compounds contained a carboxylic acid moiety, while one had an oxadiazolone ring as a carboxylic acid bioisostere – which seems necessary to obtain the activity. In the ATP binding site of *E. coli* DNA gyrase this group makes important contacts with Arg136 [31,34]. The activities of hit compounds on topo II α and *E. coli* DNA gyrase are shown in Figure 3 [29,30,32,34,38,39].

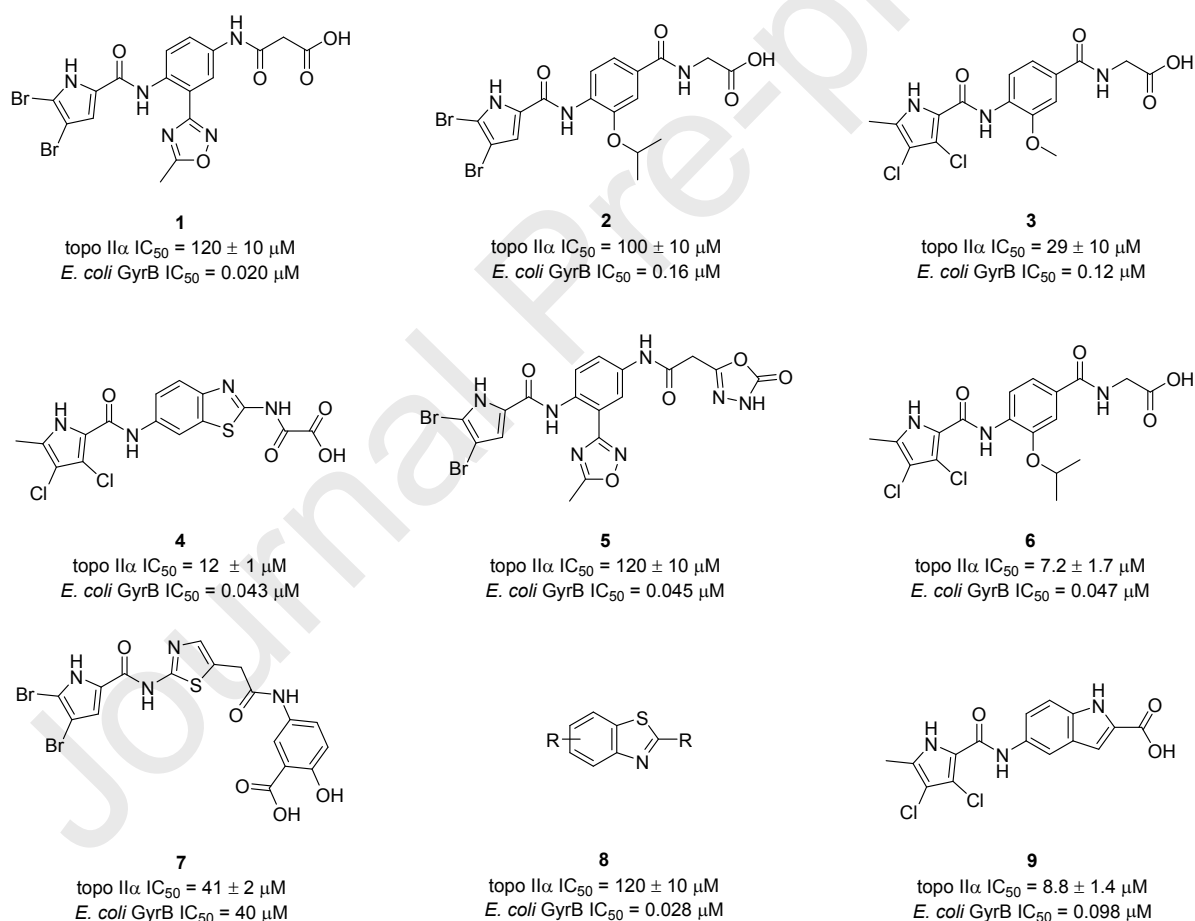


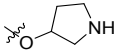
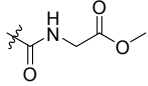
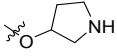
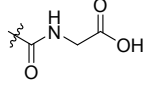
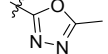
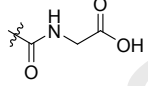
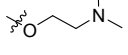
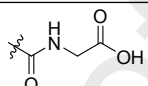
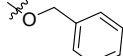
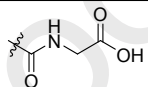
Figure 3: Structures and inhibitory activities of hit compounds identified in the initial screening on topo II α . The structure of **8** is not yet published and therefore not fully disclosed in the figure.

Because the greatest number of hits had a benzene central scaffold, and the most potent inhibitor **6** belonged to this structural type, we evaluated additional 33 benzene-type compounds from our in-house library, which provided additional 11 hits. This, more focused, screening resulted in considerably higher, 33% hit rate. Results and structures of the tested compounds **10-42** are shown in Table 1.

Table 1. Topo II α inhibitory activities of additional 33 compounds with benzene central scaffold and etoposide as positive control.

| Compound | R ^{3'} | R ^{4'} | R ^{5'} | R ² | R ³ | R ⁴ | Topo II α (μ M) |
|-----------|-----------------|-----------------|-----------------|----------------|----------------|----------------|--------------------------------|
| 10 | -Cl | -Cl | -Me | | -H | | 5.0 \pm 0.7 |
| 11 | -Cl | -Cl | -Me | | -H | | 12 \pm 1 |
| 12 | -Cl | -Cl | -Me | | -H | | 13 \pm 7 |
| 13 | -Cl | -Cl | -Me | | -H | | 26 \pm 16 |
| 14 | -H | -Br | -Br | | -H | | 34 \pm 3 |
| 15 | -Cl | -Cl | -Me | | -H | | 45 \pm 12 |
| 16 | -Cl | -Cl | -Me | | -H | | 45 \pm 14 |
| 17 | -Cl | -Cl | -Me | | -H | | 59 \pm 23 |
| 18 | -Cl | -Cl | -Me | | -H | | 63 \pm 38 |
| 19 | -Cl | -Cl | -Me | | -H | | 75 \pm 39 |

| | | | | | | | |
|----|-----|-----|-----|----|----|--|--------------------|
| 20 | -Cl | -Cl | -Me | | -H | | 86 ± 41 |
| 21 | -H | -Br | -Br | | -H | | > 100 ^a |
| 22 | -H | -Br | -Br | | -H | | > 100 |
| 23 | -H | -Br | -Br | | -H | | > 100 |
| 24 | -Cl | -Cl | -Me | | -H | | > 100 |
| 25 | -Cl | -Cl | -Me | | -H | | > 100 |
| 26 | -H | -Br | -Br | | -H | | > 100 |
| 27 | -H | -Br | -Br | | -H | | > 100 |
| 28 | -Cl | -Cl | -Me | | -H | | > 100 |
| 29 | -H | -Br | -Br | | -H | | > 100 |
| 30 | -H | -Br | -Br | | -H | | > 100 |
| 31 | -Cl | -Cl | -Me | | -H | | > 100 |
| 32 | -Cl | -Cl | -Me | | -H | | > 100 |
| 33 | -H | -Br | -Br | | -H | | > 100 |
| 34 | -H | -Br | -Br | | -H | | > 100 |
| 35 | -Cl | -Cl | -Me | -H | -H | | > 100 |

| | | | | | | | |
|------------------|-----|-----|-----|---|--|---|---------|
| 36 | -Cl | -Cl | -Me |  | -H |  | > 100 |
| 37 | -Cl | -Cl | -Me |  | -H |  | > 100 |
| 38 | -Cl | -Cl | -Me |  | -H |  | > 100 |
| 39 | -Cl | -Cl | -Me | -H |  |  | > 100 |
| 40 | -H | -Br | -Br | -H |  |  | > 100 |
| 41 | -H | -Br | -Br | -H |  |  | > 100 |
| 42 | -H | -Br | -Br | -H | OH |  | > 100 |
| Etoposide | | | | | | | 71 ± 29 |

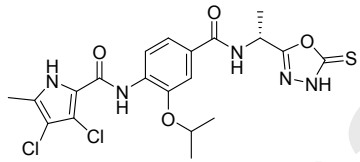
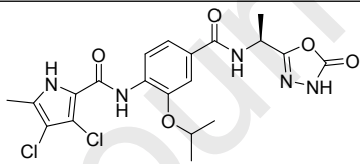
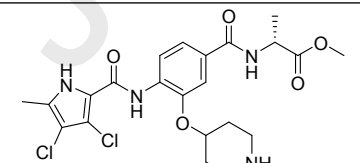
^a>100 = residual activity at 100 μ M higher than 60%.

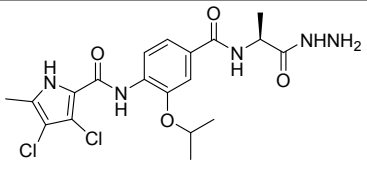
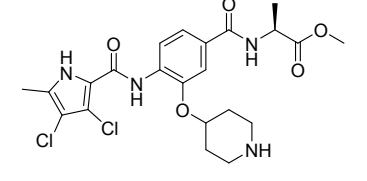
The activities of additional 33 compounds are in good agreement with the preliminary SAR of benzene-type compounds that was derived from initial screening. Analogues with dichloromethylpyrrole moiety ($R^{3'} = R^{4'} = \text{Cl}$, $R^{5'} = \text{CH}_3$; **6**, **12**) were more potent than analogues with dibromopyrrole moiety ($R^{3'} = \text{H}$, $R^{4'} = R^{5'} = \text{Br}$, **2**, **13**). As substituent R^2 , isopropoxy group seems to be preferred, however, also some alkyl or cycloalkyl substituents with basic nitrogens are tolerated, for example compound **16** with piperidinyl substituent ($\text{IC}_{50} = 45 \mu\text{M}$). Compound **35**, an analogue of **6** with hydrogen as substituent R^2 , is inactive, which indicates that larger substituents are needed in this position for tight binding. Switching the position of isopropoxy group from R^2 to R^3 also led to inactivity, as seen by comparing **6** with **39**. Out of 20 hits from initial and focused screening, 14 possess a carboxylic moiety on the right-hand side (**1**, **2**, **3**, **4**, **6**, **7**, **8**, **9**, **10**, **12**, **13**, **14**, **17**, **18**), while the rest possess a cyclic carboxylic bioisostere (**5**, **11**, **15**), ester group (**16**, **20**) or hydrazide group (**19**) at that position. Two compounds that have IC_{50} values lower than 10 μM both contain a carboxylic moiety (**6**, **10**).

All twenty hits were tested in MCF-7 breast cancer cell line (MTS assay) to evaluate their cytotoxic activity. Five compounds (**11**, **15**, **16**, **19**, **20**) showed IC_{50} values lower than 50 μM (Table 2). Those five compounds did not possess a carboxylic moiety in their structure. Even though compounds with carboxylic groups on the right-hand side generally had the best

on-target activity, they were all inactive in the cell-based assays, which suggests that the acidic nature of compounds could hinder their cell membrane permeation, making them unable to reach their target within cells. An alternative explanation is, that compounds with carboxylic moiety are better substrates of efflux pumps. Compound **11** was the only compound without carboxylic moiety in its structure that showed topo II α IC₅₀ lower than 30 μ M, while **15**, **16**, **19** and **20** only showed a moderate activity on topo II α (IC₅₀ = 45, 45, 75 and 86 μ M). Despite that, both ester group-containing compounds, **16** and **20**, had the most potent cytotoxic activity in MCF-7 cancer cell line out of all tested compounds, with IC₅₀ values lower than 10 μ M, which is significantly better than positive control etoposide (IC₅₀ = 25 μ M). Moderate on-target activity of those two compounds suggests that topo II α inhibition might not be the dominant mechanism of their cytotoxicity. Compound **20** was additionally tested in HepG2 liver cancer cell line, where it showed a similar cytotoxic activity as in MCF-7 cell line (HepG2 IC₅₀ = 10 \pm 1 μ M), and in non-cancerous human umbilical vein endothelial cell line (HUVEC), where it was inactive at 50 μ M (87% viability).

Table 2. Results of cytotoxicity testing on MCF-7 cancer cell line for compounds with viability lower than 50% at 50 μ M, and for etoposide that was used as a positive control.

| Compound | MCF-7 IC ₅₀ (μ M) |
|--|-----------------------------------|
|  <p style="text-align: center;">11</p> | 36 \pm 13 |
|  <p style="text-align: center;">15</p> | 46 \pm 16 |
|  <p style="text-align: center;">16</p> | 8.7 \pm 1.1 |

| | |
|--|---------------|
|  <p style="text-align: center;">19</p> | 19 ± 8 |
|  <p style="text-align: center;">20</p> | 8.2 ± 1.0 |
| Etoposide | 25 |

Compounds **11** and **15** share a very similar molecular structure, the only difference being their stereochemistry and the type of the bioisostere group that is attached to their right-hand sides – **11** carries an oxadiazolthione ring while **15** carries an oxadiazolone ring. While **11** has a better on-target activity, both seem to have similarly potency in MCF-7 cancer cell line, with IC_{50} values between 30 μ M and 50 μ M. Compound **19** is a derivative of **6** with carboxylic group replaced with hydrazide group. While this structural modification decreased the on-target activity by approximately ten-fold, **19** obtained a cytotoxic activity. This could, however, be associated to the well-known general toxicity of hydrazine derivatives [40].

These data therefore suggests that we have identified a novel chemotype of topo II α inhibitors, 1,2,4-substituted *N*-phenylpyrrolamides, that, depending on the nature of the substituents on the benzene ring, have potential to be optimized into potent cytotoxic agents.

2.2. Exploration of initial hits

After the identification of topo II α hit compounds that originated from the library of bacterial DNA gyrase inhibitors, a molecular docking study was performed to predict the binding poses of the inhibitors in the ATP binding site of topo II α . For docking, crystal structure of ATPase domain of topo II α in complex with AMP-PNP was used (PDB: 1ZXM). As an example, the predicted binding pose of **6** is shown in Figure 4. The pyrrolamide moiety of **6** is predicted to bind to the adenine binding pocket of the ATP binding site where its NH and CO groups form hydrogen bonds with Asn120 and a conserved water molecule. This interaction is similar to the interactions of the pyrrolamide NH with Asp73 and a conserved water molecule

that were observed in crystal structures of related compounds in ATP binding site of *E. coli* DNA gyrase [5,9]. Additionally, the interaction with Asn120 is one of the main features of known purine-like and triazinone inhibitors of topo II α [27,41]. Methyl group and halogen atoms attached to the pyrrole moiety occupy the hydrophobic pocket of the adenine binding site. Based on the docking results, it seems that the size of the hydrophobic pocket is better suited for dichloromethylpyrrole compared to dibromopyrrole, which is in good agreement with topo II α inhibition results (shown in Supporting information, Figure S3). Substituent in position four (with respect to the pyrrolamide group) on the central benzene ring forms additional contacts with some polar amino acids; the amide group is predicted to form hydrogen bonds with Asp94 and Asn150, while the terminal carboxylic moiety is predicted to form a salt bridge with Lys157. Isopropoxy group in position two is oriented towards the lipophilic part of the binding site. The substituents in position two and four occupy different binding pockets compared to known inhibitors, thus making the binding mode of this novel chemotype of ATP-competitive inhibitors of topo II α unique.

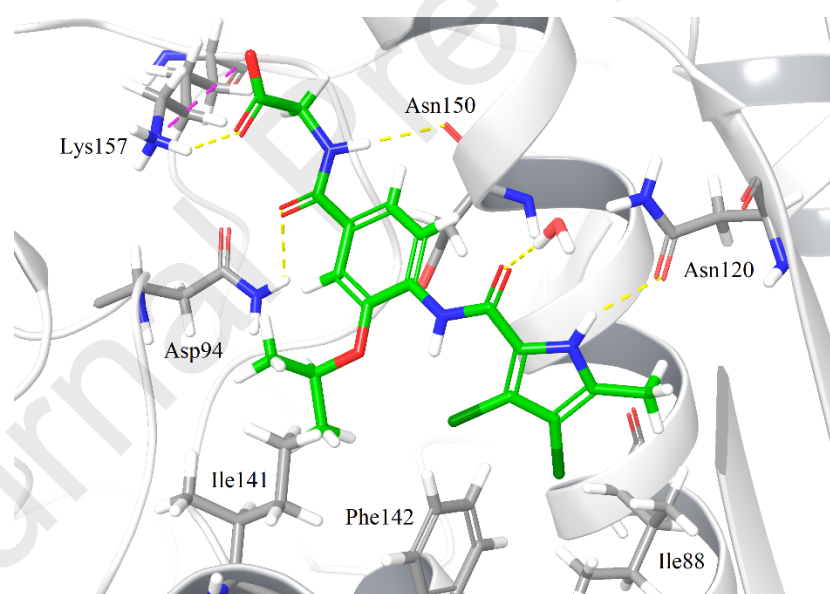


Figure 4. Predicted binding mode of **6** in ATP binding site of topo II α based on molecular docking. Main hydrogen bonds are shown in yellow dashed lines and ionic bond in purple dashed line. Also shown are amino acid residues that are forming main hydrophobic contacts.

Based on the SAR of initial inhibitors and information derived from their predicted binding poses in the active site of topo II α , we prepared a plan for further exploration of initial

hits. Our main goal was to extract the smallest required binding motif for this novel type of inhibitors. To do that, some smaller, fragment-like structures were designed in which each of the substituents on the benzene ring were systematically shortened. Because primary hits have a relatively high molecular weight and low ligand efficiency on topo II α , finding a low molecular weight inhibitor that would retain the activity of the initial hits is essential for the success of further optimization steps. In addition to improving ligand efficiency, the goal of this optimization attempt was to modify the acido-basic properties and lipophilicity of compounds to see how those modifications affect their on-target and cytotoxic activities. Because the presence of carboxylic moiety was shown to impair the cellular activity of compounds, we designed some analogues in which this functional group was absent. On the other hand, because initial hits **17** and **20**, containing a basic centre, showed the most potent cytotoxic activities, a basic heterocycle was introduced to some of the designed inhibitors. Based on these objectives, we prepared an exploration plan that is schematically presented in Figure 5.

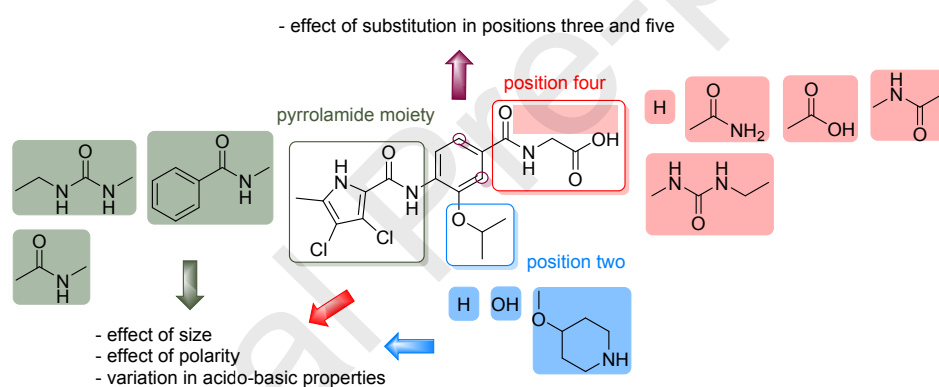


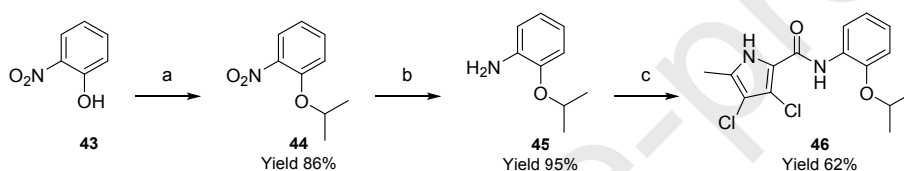
Figure 5. Schematic representation of exploration plan, based on compound **6**.

2.2.1. Synthesis

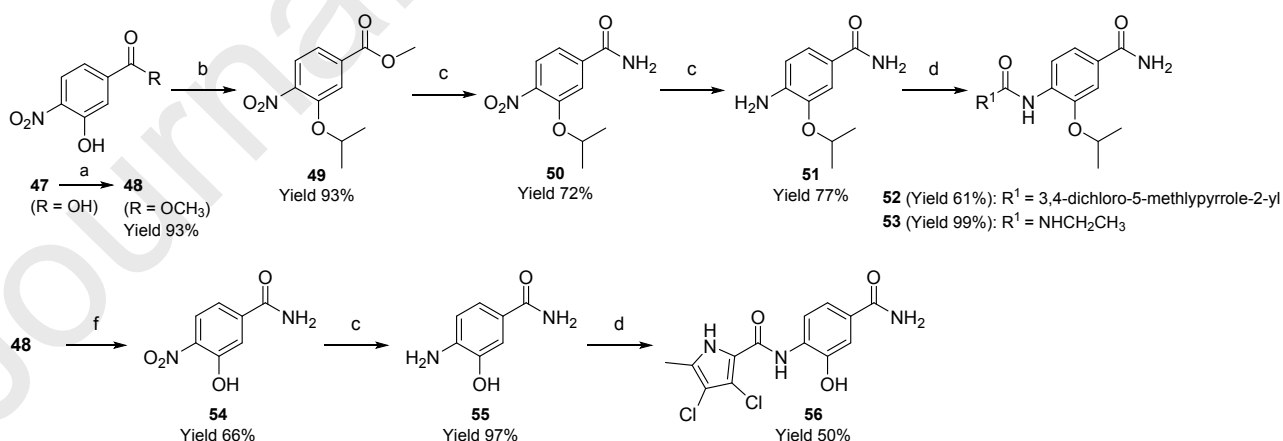
We synthesized 13 new compounds according to the synthetic pathways shown in the schemes below. Schemes 1-3 show synthesis of analogues of **6** with shorter substituents in positions two or four of the central benzene ring (**46**, **52**, **56**, **61**). Scheme 2 additionally shows synthesis of compound **53** with ethylurea group replacing the pyrrole moiety. In scheme 4, synthesis of compound **68** with the reversed amide group in position four, compared to **6**, is presented. Scheme 5 shows synthesis of **73a** with ethylurea group in position five and isopropoxy group in position two, and its derivatives **74a** with a basic heterocycle in position two, and **74b-c** with a basic heterocycle in position two and a methyl or phenyl group replacing

the pyrrole moiety. In scheme 6, synthesis of **80**, a positional isomer of compound **52**, where the isopropoxy group is attached to position three instead of position two, is presented.

Generally, the synthetic pathway started with modification of carboxyl (Fischer ester formation) or amino group (Boc protection or acylation) of the starting amino/nitro-hydroxybenzoic acid or amino/nitro-phenol, where applicable. Then Mitsunobu reaction was used to prepare the aromatic ether, which was followed by ammonolysis of ester in cases where final product had a primary amide group. Next, catalytic hydrogenation with Pd/C as the catalyst was performed to obtain aromatic amine, which was then coupled with pyrrole-2-carboxylic acid acid chloride or ethyl isocyanate. Where applicable, the final reaction constituted of Boc deprotection with 4 M HCl in dioxane or alkaline hydrolysis of ester groups.

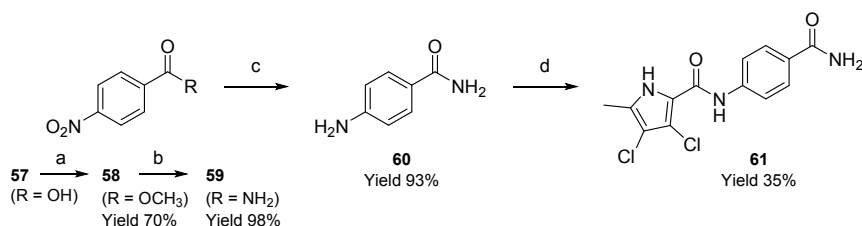


Scheme 1. Reagents and conditions: a) isopropanol, PPh₃, DIAD, THF, rt, 15h; b) H₂, Pd/C, MeOH, rt, 15 h; c) *i*: 3,4-dichloro-5-methylpyrrole-2-carboxylic acid, oxalyl chloride, anhydrous CH₂Cl₂, rt, 15 h, *ii*: anhydrous pyridine, anhydrous CH₂Cl₂, rt, 15 h.

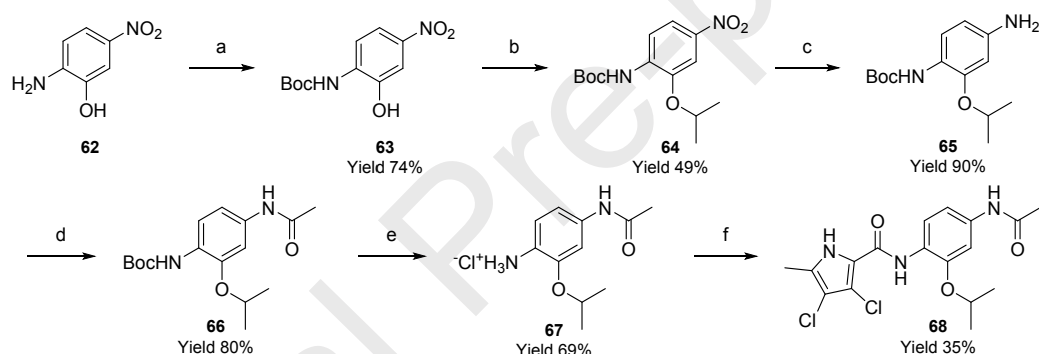


Scheme 2. Reagents and conditions: a) H₂SO₄, MeOH, reflux, 15 h; b) isopropanol, PPh₃, DIAD, THF, rt, 15 h; c) H₂, Pd/C, MeOH, rt, 3-15 h d) *i*: 3,4-dichloro-5-methylpyrrole-2-carboxylic acid, oxalyl chloride, anhydrous CH₂Cl₂, rt, 15 h, *ii*: anhydrous pyridine,

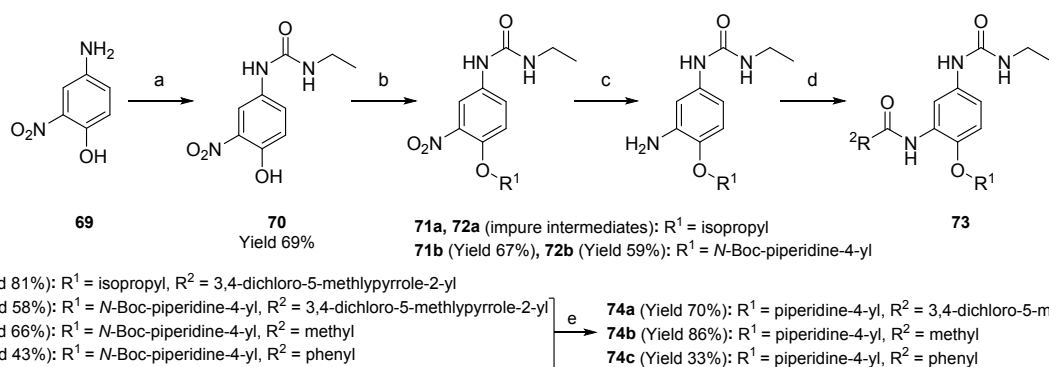
anhydrous CH_2Cl_2 , rt, 15 h (**52**, **56**) or ethyl isocyanate, CHCl_3 , rt, 15h (**53**); e) NaOH, MeOH, reflux, 5h; f) NH_3 , MeOH, 70 °C, 15 h.



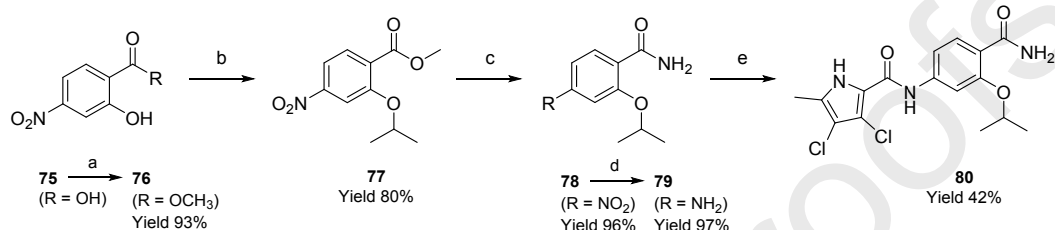
Scheme 3. Reagents and conditions: a) H_2SO_4 , MeOH, reflux, 15 h; b) NH_3 , MeOH, 70 °C, 15 h; c) H_2 , Pd/C, MeOH, rt, 15 h d) *i*: 3,4-dichloro-5-methylpyrrole-2-carboxylic acid, oxalyl chloride, anhydrous CH_2Cl_2 , rt, 15 h, *ii*: anhydrous pyridine, anhydrous CH_2Cl_2 , rt, 15 h.



Scheme 4. Reagents and conditions: a) *i*: Boc_2O , DMAP, dioxane, rt, 15 h, *ii*: 1 M NaOH, MeOH, rt, 2 h, *iii*: 1 M HCl to neutral pH; b) isopropanol, PPh_3 , DIAD, THF, rt, 15 h; c) H_2 , Pd/C, MeOH, rt, 12 h; d) acetyl chloride, Et_3N , CH_2Cl_2 , rt, 6 h; e) HCl, dioxane, rt, 15 h; f) *i*: 3,4-dichloro-5-methylpyrrole-2-carboxylic acid, oxalyl chloride, anhydrous CH_2Cl_2 , rt, 15 h, *ii*: anhydrous pyridine, anhydrous CH_2Cl_2 , rt, 15 h.



Scheme 5. Reagents and conditions: a) ethyl isocyanate, CHCl_3 , rt, 15 h; b) 1-Boc-4-hydroxypiperidine (**71a**) or 2-propanol (**71b**), PPh_3 , DIAD, THF, rt, 15 h; c) H_2 , Pd/C, MeOH, rt, 12 h; d) *i*: 3,4-dichloro-5-methylpyrrole-2-carboxylic acid, oxalyl chloride, anhydrous CH_2Cl_2 , rt, 15 h, *ii*: anhydrous pyridine, anhydrous CH_2Cl_2 , rt, 15 h (**73a, b**) or acetyl chloride, Et_3N , CH_2Cl_2 , rt, 6 h (**75c**) or benzyl chloride, Et_3N , CH_2Cl_2 , rt, 6 h (**73d**); e) HCl, dioxane, rt, 15 h.



Scheme 6. Reagents and conditions: a) H_2SO_4 , MeOH, reflux, 15 h; b) isopropanol, PPh_3 , DIAD, THF, rt, 15 h; c) NH_3 , MeOH, 70 °C, 15h; d) H_2 , Pd/C, MeOH, rt, 15h e) *i*: 3,4-dichloro-5-methylpyrrole-2-carboxylic acid, oxalyl chloride, anhydrous CH_2Cl_2 , rt, 15 h, *ii*: anhydrous pyridine, anhydrous CH_2Cl_2 , rt, 15 h.

2.2.2. *In-vitro* evaluation of the new series of compounds

Thirteen new compounds were synthesized and tested for their inhibitory activity on topo II α with relaxation assay (Table 3). Firstly, attempts were made to reduce the size of the molecule while retaining the activity and thus increasing ligand efficiency compared to the original hits. It has already been concluded that replacing the isopropoxy substituent in position two of the benzene ring with the hydrogen atom leads to inactivity (comparison of **6** to **35**). To test the importance of substituents in position four of the benzene ring, we synthesized compound **46**, an analogue of **6** with a hydrogen atom in position four. Compound **46** was inactive, showing that substitution in position four is essential for activity. Next, we prepared compound **52** with the primary amide group in position four. This compound showed a very potent topo II α inhibitory activity with IC_{50} value of 3.2 μM , indicating that the activity of compound **6** can be retained or even slightly improved with reducing the size of substituent in position four. With this change, the molecular weight dropped from 428.3 (**6**) to 370.2 (**52**) and the ligand efficiency ($\text{LE} = 1.4 \times (\text{pIC}_{50})/(\text{heavy atom count})$ [42]) increased from 0.26 (**6**) to 0.32 (**52**), therefore making the molecule easier to optimise. Further, some analogues of **52** were

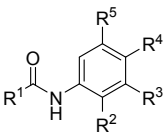
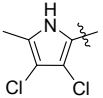
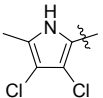
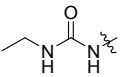
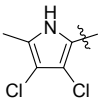
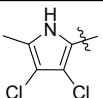
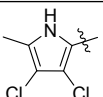
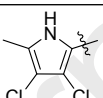
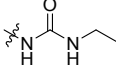
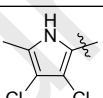
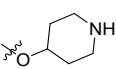
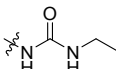
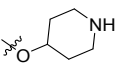
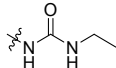
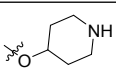
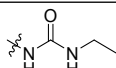
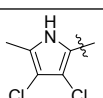
prepared: **56** and **61** in which the primary amide group was retained but hydroxyl group (**56**) or hydrogen atom (**61**) were introduced to position two; **68** in which a primary amide group was reversed as the acetamide substituent was added; and **80**, a positional isomer of **52** with isopropoxy group in position three instead of two. All these modifications resulted in the loss of activity. To assess the importance of the pyrrolamide moiety, this part of the molecule was replaced with ethylurea group (**53**), which – similarly to the pyrrolamide moiety – can bind to the adenine pocket of bacterial topoisomerases [8,43,44]. This structural modification resulted in the loss of activity.

To additionally explore the binding site, a series of compounds with the ethylurea substituent in position five was prepared. Compound **73a** with isopropoxy substituent in position two was inactive. Furthermore, derivative **74a** was synthesized, in which the isopropyl group was replaced with piperidine ring that is basic in nature, which has been proven to be beneficial for the cytotoxic activity of the initial hits **17** and **20**. Compound **74a** showed a moderate topo II α inhibitory activity with IC₅₀ value of 38 μ M. To test if the pyrrolamide moiety of **74a** is essential for the activity of this compound, we prepared **74b** and **74c** in which the pyrrole moiety was replaced with methyl or phenyl groups. Both of those compounds were inactive.

Overall, the results suggest that the pyrrolamide moiety is essential for on-target activity. Also essential is the substituent in position two, which should be bound to the phenyl ring through an oxygen atom, can carry groups with basic centres, and should not be a hydroxyl group. The substituent in position four is also crucial for activity but can be shortened to the primary amide group. The exception is compound **74a** that has moderate activity but does not contain substituents in position four but in position five.

Both active compounds (**52** and **74a**) were also evaluated for their inhibitory activities on bacterial topoisomerases DNA gyrase and topoisomerase IV from bacteria *E. coli* and *S. aureus* (Supporting information, Table S2). While their activity on *E. coli* DNA gyrase is lower than the activity of the majority of the initial hits (**1** - **20**), their IC₅₀ values on *E. coli* DNA gyrase remain about 10-fold lower than their IC₅₀ values on topo II α . The activities of these two compounds on other tested bacterial topoisomerases (*E. coli* topoisomerase IV and *S. aureus* DNA gyrase and topoisomerase IV) were weaker (IC₅₀ > 10 μ M).

Table 3. Enzymatic inhibitory activities of the synthesized compounds and etoposide as positive control.

|  | | | | | | |
|---|---|---|---|--|---|--------------------------------|
| Compound | R ¹ | R ² | R ³ | R ⁴ | R ⁵ | Topo II α (μ M) |
| 46 |  |  | -H | -H | H | > 50 μ M |
| 52 |  |  | -H |  | H | 3.2 \pm 1.8 |
| 53 |  |  | -H |  | H | > 50 μ M |
| 56 |  | -OH | -H |  | H | > 50 μ M |
| 61 |  | -H | -H |  | H | > 50 μ M |
| 68 |  |  | -H |  | H | > 50 μ M |
| 73a |  |  | -H | -H |  | > 50 μ M |
| 74a |  |  | -H | -H |  | 38 \pm 10 |
| 74b | CH ₃ |  | -H | -H |  | > 50 μ M |
| 74c | phenyl |  | -H | -H |  | > 50 μ M |
| 80 |  | -H |  | -CONH ₂ | H | > 50 μ M |
| Etoposide | | | | | | 71 \pm 29 |

Compound **52** was additionally evaluated in topo II α ATPase assays to confirm the proposed ATP-competitive mode of inhibition. The observed rates of ATP hydrolysis were plotted against ATP concentrations in the presence of **52** (0.1 μ M - 2.5 μ M), as shown in Figure 6. The graph shows that **52** decreases the rate of ATP hydrolysis, with a greater decrease at higher concentrations of **52**. The calculated K_M value increased 3-4-fold in the presence of 0.25 μ M **52** compared to no inhibitor, and increased further with inhibitor concentration (Supporting information, Table S3). The IC_{50} value determined at 2 mM ATP concentration was 0.43 ± 0.16 μ M and it steadily decreased at decreasing concentrations of ATP (Supporting information, Table S4). These data support the proposed ATP-competitive mode of topo II α inhibition.

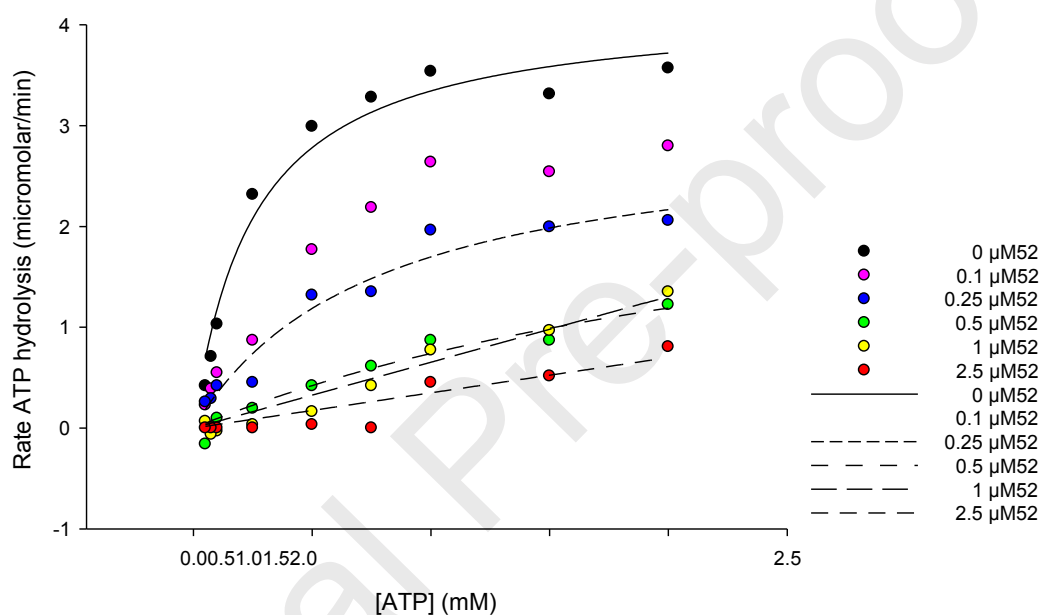
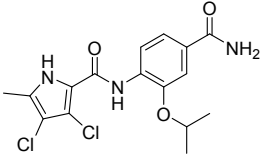
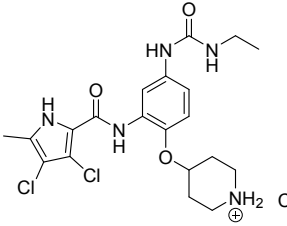


Figure 6. The rates of ATP hydrolysis plotted against ATP concentrations for compound **52**, determined using topo II α ATPase assay.

Compounds **52** and **74a** have been tested for their cytotoxicity on MCF-7 breast cancer and HepG2 liver cancer cell lines (Table 4). Compound **52** shows no cytotoxicity at 50 μ M, while **74a** shows cytotoxic activity in both tested cell lines. The IC_{50} values of **74a** against MCF-7 and HepG2 cell lines were 33 ± 4 μ M and 38 ± 8 μ M, respectively. Compound **74a** was additionally evaluated on non-cancerous HUVEC cell line, where it was inactive at 50 μ M (105% viability). The reasons for inactivity of **52** could be connected to problems with its permeability through the cell membrane or with the active efflux of compound from the cells. The activity of **74a** confirms that this molecular scaffold is useful for the design of novel cytotoxic agents, and that the presence of a basic centre is essential for the potent activity in cancer cell lines, as also seen in **17** and **20**. These findings will be used for further optimization

of this series of topo II α inhibitors, using **52** that has a very potent on-target activity and lower molecular weight as structural template.

Table 4. Results of cytotoxicity testing on MCF-7 and HepG2 cancer cell lines.

| Compound | MCF-7 IC ₅₀ (μ M) | HepG2 IC ₅₀ (μ M) |
|---|-----------------------------------|-----------------------------------|
|  <p>52</p> | > 50 | > 50 |
|  <p>74a</p> | 33 \pm 4 | 38 \pm 8 |

3. CONCLUSIONS

In this study, we have discovered a promising new class of ATP-competitive inhibitors of human DNA topoisomerase II. In-house library of ATP-competitive inhibitors of bacterial topoisomerases served us as an excellent starting point for our screening campaign. Out of twenty identified hit compounds, fifteen shared a *N*-phenylpyrrolamide scaffold, including the most potent hit **10** with IC₅₀ value of 5.0 μ M. To better understand the SAR of this new structural type of topo II α inhibitors, thirteen new compounds were designed and prepared. Two new compounds retained inhibitory activity on topo II α . Compound **52** has a potential to be used as a template for further design of topo II α inhibitors, as it has a potent inhibitory activity with an IC₅₀ value of 3.2 μ M and increased ligand efficiency compared to initial hits. With kinetic ATPase assays we confirmed the potent activity of **52** (IC₅₀ = 0.43 μ M) and its ATP-competitive mode of topo II α inhibition. All active compounds were tested for their cytotoxic activity on MCF-7 cancer cell line and selected compounds also on HepG2 cancer cell line. Six compounds showed activity in MCF-7 cancer cell line below 50 μ M and the most potent, **16** and **20**, had cytotoxic IC₅₀ values lower than 10 μ M.

4. MATERIALS AND METHODS

4.1. General chemistry information

Chemicals were obtained from Acros Organics (Geel, Belgium), Apollo Scientific (Stockport, UK), Sigma-Aldrich (St. Louis, MO, USA) and TCI (Tokyo, Japan) and were used without the preceding purification. Thin layer chromatography was performed on silica gel Merck 60 F254 plates (0.25 mm), for visualization UV light (254 nm and 366 nm) and spray reagents were used. Flash column chromatography was performed on silica gel 60 (particle size 240–400 mesh). ^1H and ^{13}C NMR spectra were recorded at 400 and 100 MHz, respectively, on a Bruker AVANCE III 400 spectrometer (Bruker Corporation, Billerica, MA, USA). To dissolve NMR samples, DMSO- d_6 or CDCl_3 (with TMS as an internal standard) were used. High resolution mass spectra were obtained using a ExactiveTM Plus Orbitrap Mass Spectrometer (Thermo Fischer Scientific, Waltham, MA, USA) or low resolution mass spectra on ADVION expression CMSL mass spectrometer (Advion, Ithaca, USA). HPLC analyses were performed on a Thermo Scientific Dionex Ultimate 3000 Binary Rapid Separation LC System (Thermo Fisher Scientific, Waltham, MA, USA), using a photodiode array detector and Agilent Zorbax 80Å Extend-C18 column (5 μm , 4.6 mm \times 150 mm). Chromeleon 7 CDC software was used to control the instrument and process the data. The eluent consisted of 0.1% TFA as solvent A and acetonitrile as solvent B. Method: 0-8 min 5% solvent B, 8-15 min 5% to 95% solvent B, 15-16 min 95% solvent B, 16-18 min 95% to 5% solvent B, 18-21 min 5% solvent B, flow rate 1.0 mL/min and sample injection volume 10 μL .

4.2. Synthetic procedures and analytical data

General procedure A. To a stirred solution of phenol (1 eq.) and triphenylphosphine (2 eq.) in anhydrous tetrahydrofuran (10 mL/mmol), alcohol (2 eq.) was added and the mixture was stirred at rt for 10 min. Diisopropyl azodicarboxylate (2 eq.) was added dropwise and the mixture was stirred at rt for 15 h under argon atmosphere. The solvent was evaporated under reduced pressure and the crude product was purified with flash column chromatography.

1-Isopropoxy-2-nitrobenzene (44) [45]. Synthesized according to General procedure A from **43** (1.00 g, 7.19 mmol) and isopropanol (5.5 mL, 71.9 mmol). Crude product was purified with flash column chromatography using hexane/ethyl acetate (2/1) as an eluent to give **44** as yellow solid. Yield 86% (1.12 g). ^1H NMR (400 MHz, CDCl_3) δ = 1.41 (d, 6H, J = 6.1 Hz, $\text{CH}(\text{CH}_3)_2$), 4.69 (hept, 1H, J = 6.1 Hz, $\text{CH}(\text{CH}_3)_2$), 7.00 (ddd, 1H, J = 8.1, 7.4, 1.2 Hz, Ar-H-4 or Ar-H-5), 7.10 (dd, 1H, J = 8.4, 1.1 Hz, Ar-H-3 or Ar-H-6), 7.50 (ddd, 1H, J = 8.5, 7.4, 1.8 Hz, Ar-H-4 or Ar-H-5), 7.78 (dd, 1H, J = 8.1, 1.7 Hz, Ar-H-3 or Ar-H-6) ppm.

General procedure B. Nitro compound (1 eq.) was dissolved in MeOH (20 mL/mmol) and the mixture was stirred for 30 min under argon atmosphere. Pd/C (20 m/m%) was added and the reaction mixture was stirred under hydrogen atmosphere for 2 h. The catalyst was filtered off and the solvent removed under reduced pressure to obtain the product.

2-Isopropoxyaniline (45) [46]. Synthesized according to General procedure B from **43** (530 mg, 2.93 mmol). Compound **45** was obtained as a colourless oil. Yield 95% (420 mg). ¹H NMR (400 MHz, CDCl₃) δ = 1.38 (d, 6H, *J* = 6.1 Hz, CH(CH₃)₂), 3.81 (s, 2H, Ar-NH₂), 4.55 (hept, 1H, *J* = 6.1 Hz, CH(CH₃)₂), 6.68 – 6.87 (m, 4H, 4 × Ar-H) ppm.

General procedure C. To a solution of 3,4-dichloro-5-methyl-1*H*-pyrrole-2-carboxylic acid (1.5 eq.) in anhydrous dichloromethane (10 mL/mmol), oxalyl chloride (7.5 eq.) was added dropwise and the mixture was stirred at room temperature for 15 h under argon atmosphere. The solvent was evaporated under reduced pressure, anhydrous dichloromethane (10 mL/mmol), amine (1 eq.) and pyridine (1 mL/mmol) were added and the reaction mixture was stirred under argon atmosphere at room temperature for 15 h. If precipitated, the product was filtered off from the reaction mixture.

3,4-Dichloro-*N*-(2-isopropoxyphenyl)-5-methyl-1*H*-pyrrole-2-carboxamide (46). Synthesized according to General procedure C from **45** (66 mg, 0.44 mmol). Crude product was suspended in hot methanol and left to cool in the refrigerator. Pure **46** was filtered off as grey solid. Yield 62% (89 mg). ¹H NMR (400 MHz, DMSO) δ = 1.33 (d, 6H, *J* = 6.0 Hz, CH(CH₃)₂), 2.23 (s, 3H, pyrrole-CH₃), 4.76 (hept, 1H, *J* = 6.0 Hz, CH(CH₃)₂), 6.95 (td, 1H, *J* = 7.8, 1.3 Hz, Ar-H-4 or Ar-H-5), 7.06 (td, 1H, *J* = 7.8, 1.6 Hz, Ar-H-4 or Ar-H-5), 7.13 (dd, 1H, *J* = 8.3, 1.3 Hz, Ar-H-3 or Ar-H-6), 8.39 (dd, 1H, *J* = 8.0, 1.6 Hz, Ar-H-3 or Ar-H-6), 9.13 (s, 1H, Ar-NHCO), 12.40 (s, 1H, pyrrole-NH) ppm. ¹³C NMR (100 MHz, DMSO-*d*₆) δ = 10.7, 21.8, 70.7, 108.4, 109.3, 112.9, 118.9, 119.0, 120.5, 123.6, 128.3, 129.3, 145.6, 156.1 ppm. HRMS for C₁₅H₁₇Cl₂N₂O₂ ([M+H]⁺): calculated 327.0662, found 327.0659. HPLC purity 100.0%.

General procedure D. To a stirring suspension of carboxylic acid (1 eq.) in methanol (2 mL/mmol), concentrated sulfuric acid (0.2 mL/mmol) was added dropwise and the mixture was refluxed overnight. Methanol was evaporated under reduced pressure, saturated NaHCO₃ was added and extracted with ethyl acetate. Organic phase was dried over Na₂SO₄, filtered and solvent was evaporated under reduced pressure.

Methyl 3-hydroxy-4-nitrobenzoate (48) [32]. Synthesized according to General procedure D from **47** (3.01 g, 16.44 mmol). Compound **48** was obtained as yellow solid. Yield

93% (3.02 g). ^1H NMR (400 MHz, DMSO) δ = 3.88 (s, 3H, COOCH_3), 7.49 (dd, 1H, J = 8.5, 1.8 Hz, Ar-H-6), 7.68 (d, 1H, J = 1.4 Hz, Ar-H-2), 7.96 (d, 1H, J = 8.2 Hz, Ar-H-5), 11.50 (s, 1H, Ar-OH) ppm.

Methyl 3-isopropoxy-4-nitrobenzoate (49) [32]. Synthesized according to General procedure A from **48** (3.00 g, 15.22 mmol) and isopropanol (2.34 mL, 30.4 mmol). The crude product was purified with flash column chromatography using hexane/ethyl acetate (5/1) as an eluent to give product as yellow oil. Yield 93% (3.64 g). ^1H NMR (400 MHz, CDCl_3) δ = 1.43 (d, 6H, J = 6.1 Hz, $\text{CH}(\text{CH}_3)_2$), 3.98 (s, 3H, COOCH_3), 4.80 (hept, 1H, J = 6.1 Hz, $\text{CH}(\text{CH}_3)_2$), 7.67 (dd, 1H, J = 8.3, 1.6 Hz, Ar-H-6), 7.76 (d, 1H, J = 1.6 Hz, Ar-H-2), 7.78 (d, 1H, J = 8.3 Hz, Ar-H-5) ppm.

General procedure E. Ester (1 eq.) was weighed into a pressure tube and dissolved in 7 M ammonia solution in methanol (10 mL/mmol; reagent commercially available from Sigma Aldrich). The solution was left to stir overnight at 70 °C after which methanol was removed under reduced pressure.

3-Isopropoxy-4-nitrobenzamide (50). Synthesized according to General procedure E from **49** (200 mg, 0.84 mmol). The product was purified with flash column chromatography using dichloromethane/methanol (9/1) as an eluent to give **53** as yellow crystals. Yield 72% (135 mg). ^1H NMR (400 MHz, DMSO) δ = 1.31 (d, 6H, J = 6.0 Hz, $\text{CH}(\text{CH}_3)_2$), 4.90 (hept, J = 6.1 Hz, $\text{CH}(\text{CH}_3)_2$), 7.55 (dd, 1H, J = 8.3, 1.6 Hz, Ar-H-6), 7.70 (bs, 1H, CONH_2 -A), 7.75 (d, 1H, J = 1.6 Hz, Ar-H-2), 7.90 (d, 1H, J = 8.3 Hz, Ar-H-5), 8.23 (bs, 1H, CONH_2 -B) ppm. ^{13}C NMR (100 MHz, $\text{DMSO}-d_6$) δ = 22.0, 72.9, 115.5, 119.9, 125.1, 139.4, 142.6, 150.2, 166.6 ppm. MS (ESI) m/z = 222.8 ($[\text{M}-\text{H}]^-$).

4-Amino-3-isopropoxybenzamide (51). Synthesized according to General procedure B from **50** (115 mg, 0.51 mmol). After removal of the solvent under reduced pressure, product was obtained as brown oil. Yield 77% (77 mg). ^1H NMR (400 MHz, DMSO) δ = 1.28 (d, 6H, J = 6.0 Hz, $\text{CH}(\text{CH}_3)_2$), 4.55 (hept, 1H, J = 6.0 Hz, $\text{CH}(\text{CH}_3)_2$), 5.29 (bs, 2H, Ar-NH₂), 6.63 (d, 1H, J = 8.2 Hz, Ar-H-5), 6.92 (bs, 1H, CONH_2 -A), 7.29 (dd, 1H, J = 8.2, 1.9 Hz, Ar-H-6), 7.35 (d, 1H, J = 1.8 Hz, Ar-H-2), 7.60 (bs, 1H, CONH_2 -B) ppm. ^{13}C NMR (100 MHz, $\text{DMSO}-d_6$) δ = 22.5, 70.7, 113.0, 113.8, 122.0, 122.0, 142.7, 143.5, 168.5 ppm. MS (ESI) m/z = 194.9 ($[\text{M}+\text{H}]^+$).

***N*-(4-Carbamoyl-2-isopropoxyphenyl)-3,4-dichloro-5-methyl-1*H*-pyrrole-2-carboxamide (52)**. Synthesized according to General procedure C from **51** (50 mg, 0.26 mmol).

The product suspended in toluene and filtered off from the reaction mixture as light grey solid. Yield 61% (58 mg). ^1H NMR (400 MHz, DMSO) δ = 1.36 (d, 6H, J = 6.0 Hz, $\text{CH}(\text{CH}_3)_2$), 2.24 (s, 3H, pyrrole, CH_3), 4.80 – 4.90 (hept, 1H, J = 5.9 Hz, $\text{CH}(\text{CH}_3)_2$), 7.34 (s, 1H, $\text{CONH}_2\text{-A}$), 7.53 (dd, 1H, J = 8.4, 1.8 Hz, Ar-H-5), 7.60 (d, 1H, J = 1.8 Hz, Ar-H-3), 7.96 (s, 1H, $\text{CONH}_2\text{-B}$), 8.44 (d, 1H, J = 8.4 Hz, Ar-H-6), 9.24 (s, 1H, Ar-NHCO), 12.46 (s, 1H, pyrrole-NH) ppm. ^{13}C NMR (100 MHz, DMSO- d_6) δ = 11.2, 22.3, 71.6, 109.1, 110.1, 112.2, 118.4, 119.2, 120.9, 129.6, 130.2, 131.4, 145.6, 156.7, 167.7 ppm. HRMS for $\text{C}_{16}\text{H}_{18}\text{Cl}_2\text{N}_3\text{O}_3$ ($[\text{M}+\text{H}]^+$): calculated 370.0720, found 370.0715. HPLC purity 96.9%.

General procedure F. To a stirring solution of amine (1 eq.) in chloroform (15 mL/mmol), cooled on ice bath, ethyl isocyanate (1.1 eq.) was added and the mixture was stirred under argon atmosphere overnight at room temperature. 20 mL of dichloromethane was added to the reaction mixture and the organic phase was washed with 1% citric acid, saturated NaHCO_3 solution and brine. Organic phase was dried over Na_2SO_4 , filtered and solvent was evaporated under reduced pressure.

4-(3-Ethylureido)-3-isopropoxybenzamide (53). Synthesized according to General procedure F from **51** (78 mg, 0.40 mmol). Pure product was filtered off directly from the reaction mixture as light brown solid. Yield 99% (105 mg). ^1H NMR (400 MHz, DMSO) δ = 1.08 (t, 3H, J = 7.2 Hz, CH_2CH_3), 1.32 (d, 6H, J = 6.0 Hz, $\text{CH}(\text{CH}_3)_2$), 3.17 – 3.05 (m, 2H, CH_2CH_3), 4.68 (hept, 1H, J = 6.0 Hz, $\text{CH}(\text{CH}_3)_2$), 7.16 (m, 2H, Ar-NH and $\text{CH}_3\text{CH}_2\text{NH}$), 7.41 (dd, 1H, J = 8.5, 1.8 Hz, Ar-H-6), 7.47 (d, 1H, J = 1.8 Hz, Ar-H-2), 7.81 (s, 2H, CONH_2), 8.18 (d, 1H, J = 8.5 Hz, Ar-H-5) ppm. ^{13}C NMR (100 MHz, DMSO- d_6) δ = 15.7, 22.3, 34.3, 71.4, 112.8, 117.0, 120.9, 126.8, 134.1, 144.9, 155.2, 168.0 ppm. HRMS for $\text{C}_{13}\text{H}_{20}\text{N}_3\text{O}_3$ ($[\text{M}+\text{H}]^+$): calculated 266.1499, found 266.1498. HRMS for $\text{C}_{13}\text{H}_{20}\text{N}_3\text{O}_3$ ($[\text{M}+\text{H}]^+$): calculated 266.1499, found 266.1498. HPLC purity 99.2%.

3-Hydroxy-4-nitrobenzamide (54). Compound **48** (8.5 g, 43.1 mmol) was dissolved in 100 mL of 25% aqueous ammonia solution and was stirred at 80°C overnight. The reaction mixture was acidified with concentrated HCl after which the formed precipitate was filtered off. The precipitate was dissolved in 500 mL of ethyl acetate and washed with saturated NaHCO_3 solution. After removal of the solvent under reduced pressure, product was obtained as yellow solid. Yield 66% (5.20 g). ^1H NMR (400 MHz, DMSO) δ = 7.41 (dd, 1H, J = 8.5, 1.8 Hz, Ar-H-6), 7.57 (d, 1H, J = 1.7 Hz, Ar-H-2), 7.62 (s, 1H, $\text{CONH}_2\text{-A}$), 7.93 (d, 1H, J = 8.5

Hz, Ar-H-5), 8.14 (s, 1H, CONH₂-B), 11.19 (s, 1H, Ar-OH) ppm. ¹³C NMR (100 MHz, DMSO-*d*₆) δ = 118.3, 118.8, 125.6, 139.0, 140.5, 152.0, 166.7 ppm. MS (ESI) *m/z* = 180.8 ([M-H]⁻).

4-Amino-3-hydroxybenzamide (55). Synthesized according to General procedure B from **54** (169 mg, 0.97 mmol). After removal of the solvent under reduced pressure, product was obtained as brown oil. Yield 97% (143 mg). ¹H NMR (400 MHz, DMSO) δ = 5.04 (s, 2H, Ar-NH₂), 6.54 (d, 1H, *J* = 8.1 Hz, Ar-H-5), 6.81 (bs, 1H, CONH₂-A), 7.16 (dd, 1H, *J* = 8.1, 2.0 Hz, Ar-H-6), 7.20 (d, 1H, *J* = 2.0 Hz, Ar-H-2), 7.48 (bs, 1H, CONH₂-B), 9.17 (s, 1H, Ar-OH) ppm. MS (ESI) *m/z* = 150.8 ([M-H]⁻).

***N*-(4-Carbamoyl-2-hydroxyphenyl)-3,4-dichloro-5-methyl-1*H*-pyrrole-2-carboxamide (56).** Synthesized according to General procedure C from **55** (66 mg, 0.43 mmol). The product was filtered off from the reaction mixture as off-white solid. Yield 50% (55 mg). ¹H NMR (400 MHz, DMSO) δ = 2.24 (s, 3H, pyrrole-CH₃), 7.23 (s, 1H, CONH₂-A), 7.39 (dd, 1H, *J* = 8.4, 2.0 Hz, Ar-H-5), 7.46 (d, 1H, *J* = 2.0 Hz, Ar-H-3), 7.86 (s, 1H, CONH₂-B), 8.30 (d, 1H, *J* = 8.4, Ar-H-6), 9.17 (s, 1H, Ar-OH or Ar-NH), 10.69 (s, 1H, Ar-OH or Ar-NH), 12.44 (s, 1H, pyrrole-NH) ppm. ¹³C NMR (100 MHz, DMSO-*d*₆) δ = 11.2, 109.1, 110.4, 114.5, 118.7, 119.2, 119.2, 129.7, 129.9, 130.0, 146.1, 156.8, 168.0 ppm. HRMS for C₁₃H₁₂Cl₂N₃O₃ ([M+H]⁺): calculated 328.0250, found 328.0251. HPLC purity 96.9%.

Methyl 4-nitrobenzoate (58) [47]. Synthesized according to General procedure D from **57** (3.00 g, 18.0 mmol). Pure product was filtered off directly from the reaction mixture after cooling down as yellow solid. Yield 70% (2.27 g). ¹H NMR (400 MHz, DMSO) δ = 3.93 (s, 3H, COOCH₃), 8.20 (d, 2H, *J* = 9.1 Hz, 2 × Ar-H), 8.36 (d, 2H, *J* = 9.0 Hz, 2 × Ar-H) ppm.

4-Nitrobenzamide (59) [48]. Synthesized according to General procedure E from **58** (1.20 g, 6.62 mmol). Product was obtained as yellow solid. Yield 98% (1.08 g). ¹H NMR (400 MHz, DMSO) δ = 7.75 (bs, 1H, CONH₂-A), 8.07 – 8.14 (m, 2H, 2 × Ar-H), 8.26 – 8.36 (m 3H, 2 × Ar-H and CONH₂-B) ppm.

4-Aminobenzamide (60) [49]. Synthesized according to General procedure B from **59** (430 mg, 2.59 mmol). Product was obtained as colourless oil. Yield 93% (328 mg). ¹H NMR (400 MHz, DMSO) δ = 5.60 (s, 2H, Ar-NH₂), 6.52 (d, 2H, *J* = 8.7 Hz, 2 × Ar-H), 6.84 (s, 1H, CONH₂-A), 7.51 (s, 1H, CONH₂-B), 7.58 (d, 2H, *J* = 8.7 Hz, 2 × Ar-H) ppm.

***N*-(4-Carbamoylphenyl)-3,4-dichloro-5-methyl-1*H*-pyrrole-2-carboxamide (61).** Synthesized according to General procedure C from **60** (80 mg, 0.59 mmol). Crude product was

suspended in ethyl acetate and pure **61** was filtered off as a brown solid. Yield 35% (64 mg). ^1H NMR (400 MHz, DMSO) δ = 2.24 (s, 3H, pyrrole- CH_3), 7.29 (s, 1H, $\text{CONH}_2\text{-A}$), 7.73 (d, 2H, J = 8.8 Hz, $2 \times \text{Ar-H}$), 7.87 (d, 2H, J = 8.7 Hz, $2 \times \text{Ar-H}$), 7.90 (s, 1H, $\text{CONH}_2\text{-B}$), 9.65 (s, 1H, Ar- NHCO), 12.24 (s, 1H, pyrrole-NH) ppm. ^{13}C NMR (100 MHz, DMSO- d_6) δ = 10.8, 108.6, 111.7, 118.9, 119.4, 128.3, 128.3, 129.0, 141.2, 157.3, 167.3 ppm. HRMS for $\text{C}_{13}\text{H}_{12}\text{Cl}_2\text{N}_3\text{O}_2$ ($[\text{M}+\text{H}]^+$): calculated 312.0301, found 312.0302. HPLC purity 94.2%.

tert-Butyl (2-hydroxy-4-nitrophenyl)carbamate (63) [50]. To a solution of **62** (5.00 g, 32.4 mmol) in dioxane (70 mL) di-*tert*-butyl dicarbonate (14.16 g, 38.93 mmol) and 4-dimethylaminopyridine (150 mg, 64.9 mmol) were added and the mixture was stirred overnight at room temperature. The solvent was evaporated under reduced pressure, the residue was dissolved in ethyl acetate (100 mL) and washed with 1% citric acid, water and brine. Organic phase was dried over Na_2SO_4 , filtered and solvent was evaporated under reduced pressure. Then toluene (100 mL) was added and the suspension was refluxed for 1 h, after which it was cooled down. The product was filtered off as brown crystals. Yield 74% (6.11 g). ^1H NMR (400 MHz, DMSO): δ = 1.49 (s, 9H, $3 \times \text{CH}_3$), 7.60 (d, 1H, J = 2.6 Hz, Ar-H-3), 7.70 (dd, 1H, J = 9.0, 2.6 Hz, Ar-H-5), 8.01 (d, 1H, J = 9.0 Hz, Ar-H-6), 8.27 (s, 1H, Ar-OH or NHBoc) ppm, Ar-OH or NHBoc not visible.

tert-Butyl (2-isopropoxy-4-nitrophenyl)carbamate (64). Synthesized according to General procedure A from **63** (509 mg, 2.00 mmol) and isopropanol (0.31 mL, 4.00 mmol). Crude product was purified with flash column chromatography using hexane/ethyl acetate (4/1) as an eluent to give **64** as yellow solid. Yield 49% (292 mg). ^1H NMR (400 MHz, DMSO) δ = 1.34 (d, 6H, J = 6.0 Hz, $\text{CH}(\text{CH}_3)_2$), 1.50 (s, 9H, $3 \times \text{CH}_3$), 4.85 (hept, 1H, J = 6.0 Hz, $\text{CH}(\text{CH}_3)_2$), 7.77 (d, 1H, J = 2.5 Hz, Ar-H-3), 7.85 (dd, 1H, J = 9.0, 2.5 Hz, Ar-H-5), 8.12 (d, 1H, J = 9.0 Hz, Ar-H-6), 8.33 (s, 1H, NHBoc) ppm. ^{13}C NMR (100 MHz, DMSO- d_6) δ = 21.3, 27.9, 71.4, 80.7, 107.3, 116.6, 117.9, 135.3, 142.0, 145.9, 152.1 ppm. MS (ESI) m/z = 295.0 ($[\text{M}-\text{H}]^-$).

tert-Butyl (4-amino-2-isopropoxyphenyl)carbamate (65). Synthesized according to General procedure B from **64** (261 mg, 0.88 mmol). The crude product was purified with flash column chromatography using hexane/ethyl acetate (1/1) as an eluent to give **65** as light brown oil. Yield 90% (211 mg). ^1H NMR (400 MHz, CDCl_3) δ = 1.36 (d, 6H, J = 6.1 Hz, $\text{CH}(\text{CH}_3)_2$), 1.53 (s, 9H, $3 \times \text{CH}_3$), 3.51 (s, 2H, NH_2), 4.50 (hept, 1H, J = 6.1 Hz, $\text{CH}(\text{CH}_3)_2$), 6.26 – 6.31 (m, 2H, $2 \times \text{Ar-H}$), 6.78 (bs, 1H, Ar-H or NHBoc), 7.82 (bs, 1H, Ar-H or NHBoc) ppm. ^{13}C

NMR (100 MHz, CDCl₃) δ = 22.2, 28.4, 71.0, 79.8, 101.2, 107.4, 119.9, 120.8, 141.9, 147.1, 153.1 ppm. MS (ESI) m/z = 267.0 ([M+H]⁺).

tert-Butyl (4-acetamido-2-isopropoxyphenyl)carbamate (66). To a stirring solution of **65** (331 mg, 1.24 mmol) in dichloromethane (20 mL), cooled on ice bath, acetic anhydride (0.705 mL, 7.46 mmol) was added and the mixture was stirred under argon atmosphere overnight at room temperature. 10 mL of dichloromethane was added to the reaction mixture and the organic phase was washed with saturated NaHCO₃ solution and brine. Organic phase was dried over Na₂SO₄, filtered and solvent was evaporated under reduced pressure to give product as brown solid. Yield 80% (307 mg). ¹H NMR (400 MHz, DMSO) δ = 1.38 (d, 6H, J = 6.1 Hz, CH(CH₃)₂), 1.54 (s, 9H, C(CH₃)₃), 2.17 (s, 3H, NHCOCH₃), 4.61 (m, 1H, CH(CH₃)₂), 6.66 (dd, 1H, J = 8.8, 2.2 Hz, Ar-H-5), 7.00 (s, 1H, Ar-NH), 7.26 (s, 1H, Ar-NH), 7.59 (d, 1H, J = 1.8 Hz, Ar-H-3), δ 8.01 (d, 1H, J = 8.8 Hz, Ar-H-6) ppm. MS (ESI) m/z = 309.0 ([M+H]⁺).

General procedure G. To a stirring solution of Boc-protected compound (1 eq.) in dioxane (8 mL/mmol), 4 M HCl in dioxane (10 eq.) was added and the mixture was left to stir overnight at room temperature. Product was filtered off from reaction mixture.

4-Acetamido-2-isopropoxybenzenaminium chloride (67). Synthesized according to General procedure G from **66** (290 mg, 0.94 mmol). Product was obtained as a white solid. Yield 69% (158 mg). ¹H NMR (400 MHz, DMSO) δ = 1.33 (d, 6H, J = 6.0 Hz, CH(CH₃)₂), 2.05 (s, 3H, NHCOCH₃), 4.53 – 4.65 (m, 1H, CH(CH₃)₂), 7.14 (dd, 1H, J = 8.6, 2.0 Hz, Ar-H-5), 7.27 (d, 1H, J = 8.5 Hz, Ar-H-6), 7.52 (d, 1H, J = 1.9 Hz, Ar-H-3), 10.22 (s, 1H, NHCOCH₃) ppm, NH₃⁺ not visible. ¹³C NMR (100 MHz, DMSO-*d*₆) δ = 22.1, 24.5, 71.6, 105.4, 111.1, 116.1, 124.5, 140.7, 160.0, 169.1 ppm. MS (ESI) m/z = 209.0 ([M+H]⁺).

N-(4-Acetamido-2-isopropoxyphenyl)-3,4-dichloro-5-methyl-1H-pyrrole-2-carboxamide (68). Synthesized according to General procedure C from **67** (71 mg, 0.29 mmol). The product was purified by precipitation in 1 M HCl (10 mL) and a few drops of THF and was filtered off as a brown solid. Yield 35% (39 mg). ¹H NMR (400 MHz, DMSO) δ = 1.35 (d, 6H, J = 6.0 Hz, CH(CH₃)₂), 2.03 (s, 3H, pyrrole-CH₃ or NHCOCH₃), 2.22 (s, 3H, pyrrole-CH₃ or NHCOCH₃), 4.52 – 4.69 (m, 1H, CH(CH₃)₂), 7.07 (dd, 1H, J = 8.8, 2.1 Hz, Ar-H-5), 7.51 (d, 1H, J = 2.0 Hz, Ar-H-3), 8.27 (d, 1H, J = 8.8 Hz, Ar-H-6), 9.01 (s, 1H, Ar-NH), 9.94 (s, 1H, Ar-NH), 12.35 (s, 1H, pyrrole-NH) ppm. ¹³C NMR (100 MHz, DMSO-*d*₆) δ = 11.2, 22.3, 24.5, 71.5, 104.9, 108.8, 109.6, 111.3, 119.4, 119.6, 124.0, 129.6, 136.0, 146.2, 156.3, 168.6 ppm.

HRMS for $C_{17}H_{18}Cl_2N_3O_3$ ($[M-H]^-$): calculated 382.0731, found 482.0733. HRMS for $C_{17}H_{18}Cl_2N_3O_3$ ($[M-H]^-$): calculated 382.0731, found 382.0733. HPLC purity 95.4%.

1-Ethyl-3-(4-hydroxy-3-nitrophenyl)urea (70). Synthesized according to General procedure F from **69** (809 mg, 5.25 mmol). The product was filtered directly from reaction mixture as green solid. Yield 69% (813 mg). 1H NMR (400 MHz, DMSO) δ = 1.05 (t, 3H, J = 7.2 Hz, CH_2CH_3), 3.10 (qd, 2H, J = 7.1, 5.6 Hz, CH_2CH_3), 6.17 (t, 1H, J = 5.6 Hz, $NHCH_2CH_3$), 7.02 (d, 1H, J = 8.9 Hz, Ar-H-5), 7.43 (dd, 1H, J = 9.0, 2.7 Hz, Ar-H-6), 8.14 (d, 1H, J = 2.7 Hz, Ar-H-2), 8.58 (s, 1H, Ar-OH or Ar-NHCO), 9.27 (s, 1H, Ar-OH or Ar-NHCO) ppm. ^{13}C NMR (100 MHz, DMSO- d_6) δ = 15.4, 34.0, 112.9, 119.4, 126.1, 132.7, 135.6, 146.9, 155.1 ppm. MS (ESI) m/z = 223.9 ($[M-H]^-$).

1-Ethyl-3-(4-isopropoxy-3-nitrophenyl)urea (71a). Synthesized according to General procedure A from **70** (300 mg, 1.33 mmol) and isopropanol (1.02 mL, 13.3 mmol). Crude product was purified with flash column chromatography using dichloromethane/methanol (20/1) as an eluent to give impure product as brown oil. Impure product was used in the next synthetic step without further purification. Yield /. 1H NMR (400 MHz, DMSO) δ = 1.05 (t, 3H, J = 7.2 Hz, CH_2CH_3), 1.26 (d, 6H, J = 6.1 Hz, $CH(CH_3)_2$), 3.10 (qd, 2H, J = 7.2, 5.6 Hz, CH_2CH_3), 4.66 (hept, 1H, J = 6.0 Hz, $CH(CH_3)_2$), 6.19 (t, 1H, J = 5.6 Hz, $NHCH_2$), 7.27 (d, 1H, J = 9.2 Hz, Ar-H-5), 7.47 (dd, 1H, J = 9.1, 2.7 Hz, Ar-H-6), 8.02 (d, 1H, J = 2.7 Hz, Ar-H-2), 8.65 (s, 1H, Ar-NH) ppm. MS (ESI) m/z = 265.9 ($[M-H]^-$).

tert-Butyl 4-(4-(3-ethylureido)-2-nitrophenoxy)piperidine-1-carboxylate (71b). Synthesized according to General procedure A from **70** (224 mg, 0.99 mmol) and *tert*-butyl 4-hydroxypiperidine-1-carboxylate (200 mg, 0.99 mmol). Crude product was purified with flash column chromatography using dichloromethane/methanol (40/1) as an eluent to give product as brown solidified oil. Yield 67% (272 mg). 1H NMR (400 MHz, $CDCl_3$) δ = 1.16 (t, 3H, J = 7.2 Hz, CH_2CH_3), 1.48 (d, 9H, J = 3.2 Hz, $OC(CH_3)_3$), 1.74 – 1.91 (m, 4H, $2 \times$ piperidine- CH_2), 3.29 (qd, 2H, J = 7.2, 5.5 Hz, CH_2CH_3), 3.48 (m, 2H, piperidine- CH_2), 3.56 (m, 2H, piperidine- CH_2), 4.57 (tt, 1H, J = 6.3, 3.4 Hz, piperidine-CH), 5.47 (t, 1H, J = 5.5 Hz, $NHCH_2CH_3$), 6.98 (d, 1H, J = 9.2 Hz, Ar-H-6), 7.58 (dd, 1H, J = 9.1, 2.8 Hz, Ar-H-5), 7.65 (s, 1H, Ar-NHCO), 7.72 (d, 1H, J = 2.7 Hz Ar-H-3) ppm. ^{13}C NMR (100 MHz, $CDCl_3$) δ = 15.4, 28.5, 34.1, 35.0, 67.9, 74.2, 80.0, 116.4, 117.5, 125.3, 133.1, 140.7, 145.7, 155.0, 155.9 ppm. MS (ESI) m/z = 407.1 ($[M-H]^-$).

1-(3-Amino-4-isopropoxyphenyl)-3-ethylurea (72a). Synthesized according to General procedure B from impure **71a**. The crude product was purified with flash column chromatography using dichloromethane/methanol (20/1) as an eluent to give product as brown solidified oil. Yield - (percentage not calculated because of impure starting material; 81 mg). ^1H NMR (400 MHz, DMSO) δ = 1.02 (t, 3H, J = 7.2 Hz, CH_2CH_3), 1.21 (d, 6H, J = 6.1 Hz, $\text{CH}(\text{CH}_3)_2$), 3.06 (qd, 2H, J = 7.2, 5.6 Hz, CH_2CH_3), 4.29 (hept, 1H, J = 6.1 Hz, $\text{CH}(\text{CH}_3)_2$), 4.58 (s, 2H, NH_2), 5.87 (t, 1H, J = 5.6 Hz, NHCH_2CH_3), 6.47 (dd, 1H, J = 8.6, 2.6 Hz, Ar-H-6), 6.63 (d, 1H, J = 8.6 Hz, Ar-H-5), 6.72 (d, 1H, J = 2.6 Hz, Ar-H-2), 7.93 (s, 1H, Ar-NHCO) ppm. ^{13}C NMR (100 MHz, DMSO- d_6) δ = 15.5, 22.1, 33.8, 70.8, 105.1, 106.1, 115.7, 134.6, 139.0, 139.1, 155.3 ppm. MS (ESI) m/z = 238.9 ($[\text{M}+\text{H}]^+$).

tert-Butyl 4-(2-amino-4-(3-ethylureido)phenoxy)piperidine-1-carboxylate (72b). Synthesized according to General procedure B from **71b** (260 mg, 0.64 mmol). The crude product was purified with flash column chromatography using ethyl acetate/hexane (13/1) as an eluent to give product as yellow solidified oil. Yield 59% (142 mg). ^1H NMR (400 MHz, DMSO) δ = 1.02 (t, 3H, J = 7.2 Hz, CH_2CH_3), 1.48 – 1.62 (m, 2H, piperidine- CH_2), 1.73 – 1.88 (m, 2H, piperidine- CH_2), 3.11 – 3.22 (m, 4H, CH_2CH_3 and piperidine- CH_2), 3.59 – 3.75 (m, 2H, piperidine- CH_2), 4.25 (tt, 1H, J = 7.6, 3.6 Hz, piperidine-CH), 4.67 (s, 2H, NH_2), 5.89 (t, 1H, J = 5.6 Hz, NHCH_2CH_3), 6.47 (dd, 1H, J = 8.6, 2.5 Hz, Ar-H-5), 6.67 (d, 1H, J = 8.6 Hz, Ar-H-6), 6.73 (d, 1H, J = 2.6 Hz, Ar-H-3), 7.96 (s, 1H, Ar-NHCO) ppm. ^{13}C NMR (100 MHz, CDCl_3) δ = 15.5, 28.5, 30.8, 34.9, 40.6, 73.6, 79.8, 109.4, 111.4, 115.0, 132.9, 138.1, 141.0, 154.9, 156.8 ppm. MS (ESI) m/z = 377.1 ($[\text{M}-\text{H}]^-$).

3,4-Dichloro-N-(5-(3-ethylureido)-2-isopropoxyphenyl)-5-methyl-1H-pyrrole-2-carboxamide (73a). Synthesized according to General procedure C from **72a** (61 mg, 0.26 mmol). The product was filtered off directly from the reaction mixture as beige solid. Yield 81% (86 mg). ^1H NMR (400 MHz, DMSO) δ = 1.05 (t, 3H, J = 7.2 Hz, CH_2CH_3), 1.30 (d, 6H, J = 6.0 Hz, $\text{CH}(\text{CH}_3)_2$), 2.24 (s, 3H, pyrrole- CH_3), 3.10 (qd, 2H, J = 7.2, 5.5 Hz, CH_2CH_3), 4.64 (hept, 1H, J = 6.1 Hz, $\text{CH}(\text{CH}_3)_2$), 5.95 (t, 1H, J = 5.6 Hz, NHCH_2CH_3), 6.99 (d, 1H, J = 9.1 Hz, Ar-H-6), 7.27 (dd, 1H, J = 8.9, 2.6 Hz, Ar-H-5), 8.28 (d, 1H, J = 2.6 Hz, Ar-H-3), 8.34 (s, 1H, Ar-NH), 9.08 (s, 1H, Ar-NH), 12.33 (s, 1H, pyrrole-NH) ppm. ^{13}C NMR (100 MHz, DMSO- d_6) δ = 11.2, 16.0, 22.4, 34.4, 71.7, 108.9, 110.3, 113.7, 114.2, 119.4, 128.9, 129.7, 134.3, 140.7, 155.8, 156.4 ppm. HRMS for $\text{C}_{18}\text{H}_{21}\text{Cl}_2\text{N}_4\text{O}_3$ ($[\text{M}-\text{H}]^-$): calculated 411.0991, found 411.0996. HPLC purity 98.5%.

tert-Butyl 4-(2-(3,4-dichloro-5-methyl-1H-pyrrole-2-carboxamido)-4-(3-ethylureido)phenoxy)piperidine-1-carboxylate (73b). Synthesized according to General procedure C from **72b** (110 mg, 0.29 mmol). The solvent was evaporated under reduced pressure, the residue was dissolved in ethyl acetate (100 mL) and washed with 1% citric acid, saturated NaHCO₃ solution and brine. Organic phase was dried over Na₂SO₄, filtered and solvent was evaporated under reduced pressure. The product was purified by precipitation in toluene (10 mL) and was filtered off as light brown solid. Yield 58% (95 mg). ¹H NMR (400 MHz, DMSO) δ = 1.05 (t, 3H, *J* = 7.2 Hz, CH₂CH₃), 1.41 (s, 9H, OC(CH₃)₃), 1.43 – 1.57 (m, 2H, piperidine-CH₂), 1.98 (m, 2H, piperidine-CH₂), 2.24 (s, 3H, pyrrole-CH₃), 2.97 – 3.17 (m, 4H, CH₂CH₃ and piperidine-CH₂), 3.73 – 3.87 (m, 2H, piperidine-CH₂), 4.55 (tt, 1H, *J* = 8.9, 3.9 Hz, piperidine-CH), 5.96 (t, 1H, *J* = 5.6 Hz, NHCH₂CH₃), 7.06 (d, 1H, *J* = 9.1 Hz, Ar-H-6), 7.29 (dd, 1H, *J* = 8.9, 2.6 Hz, Ar-H-5), 8.26 (d, 1H, *J* = 2.6 Hz, Ar-H-3), 8.37 (s, 1H, Ar-NH), 8.97 (s, 1H, Ar-NH), 12.33 (s, 1H, pyrrole-NH) ppm. ¹³C NMR (100 MHz, CDCl₃) δ = 10.7, 15.5, 28.0, 30.7, 33.9, 74.2, 78.8, 108.4, 109.2, 110.0, 113.2, 114.0, 118.9, 128.3, 129.3, 134.1, 140.0, 153.9, 155.2, 156.0 ppm. HRMS for C₂₅H₃₄Cl₂N₅O₅ ([M+H]⁺): calculated 554.1932, found 554.1924 HPLC purity 98.1%.

tert-Butyl 4-(2-acetamido-4-(3-ethylureido)phenoxy)piperidine-1-carboxylate (73c). To a stirring solution of **72b** (80 mg, 0.21 mmol) and triethylamine (0.035 mL, 0.25 mmol) in dichloromethane (10 mL), cooled on ice bath, acetyl chloride (0.017 mL, 0.23 mmol) was added and the mixture was stirred under argon atmosphere overnight at room temperature. 10 mL of dichloromethane was added to the reaction mixture and the organic phase was washed with 10% citric acid, saturated NaHCO₃ solution and brine. Organic phase was dried over Na₂SO₄, filtered and solvent was evaporated under reduced pressure to give product as light brown crystals. Yield 66% (59 mg). ¹H NMR (400 MHz, CDCl₃) δ = 1.08 (t, 3H, *J* = 7.3, CH₂CH₃), 1.47 (s, 9H, OC(CH₃)₃), 1.61 – 1.78 (m, 2H, piperidine-CH₂), 1.94 (bs, 2H, piperidine-CH₂), 2.18 (s, 3H, NHCOCH₃), 3.15 – 3.29 (m, 4H, CH₂CH₃ and piperidine-CH₂), 3.67 – 3.88 (m, 2H, piperidine-CH₂), 4.32 – 4.46 (m, 1H, piperidine-CH), 5.47 (bs, 1H, NHCH₂CH₃), 6.79 (d, 1H, *J* = 8.8 Hz, Ar-H-6), 7.30 – 7.43 (m, 2H, Ar-H-3 and Ar-H-5), 7.82 (s, 1H, Ar-NH), 7.98 (s, 1H, Ar-NH) ppm. ¹³C NMR (100 MHz, CDCl₃) δ = 15.4, 24.9, 28.4, 30.8, 34.9, 41.0, 113.3, 113.8, 116.4, 128.6, 133.1, 141.4, 154.7, 156.5, 168.5 ppm. MS (ESI) *m/z* = 419.2 ([M-H]⁻).

tert-Butyl 4-(2-benzamido-4-(3-ethylureido)phenoxy)piperidine-1-carboxylate (73d). To a stirring solution of **72b** (70 mg, 0.19 mmol) and triethylamine (0.031 mL, 0.22

mmol) in dichloromethane (10 mL), cooled on ice bath, benzoyl chloride (0.024 mL, 0.20 mmol) was added and the mixture was stirred under argon atmosphere overnight at room temperature. The solvent was evaporated under reduced pressure and the crude product was purified with flash column chromatography using dichloromethane/methanol (20/1) as an eluent to give product as yellow oil. Yield 43% (38 mg). ^1H NMR (400 MHz, DMSO) δ = 1.05 (t, 3H, J = 7.1 Hz, CH_2CH_3), 1.38 (s, 9H, $\text{OC}(\text{CH}_3)_3$), 1.54 – 1.70 (m, 2H, piperidine- CH_2), 1.81 – 1.91 (m, 2H, piperidine- CH_2), 3.06 – 3.14 (m, 2H, CH_2CH_3), 3.14 – 3.25 (m, 2H, piperidine- CH_2), 3.54 – 3.64 (m, 2H, piperidine- CH_2), 4.43 – 4.52 (m, 1H, piperidine-CH), 5.97 (t, 1H, J = 5.6 Hz, NHCH_2CH_3), 7.02 (d, 1H, J = 9.0 Hz, Ar-H), 7.26 (dd, 1H, J = 8.9, 2.7 Hz, Ar-H), 7.50 – 7.64 (m, 3H, $3 \times$ Ar-H), 7.83 – 7.93 (m, 2H, $2 \times$ Ar-H), 7.92 (dd, 1H, J = 8.4, 1.4 Hz, Ar-H), 8.36 (s, 1H, Ar-NH), 9.37 (s, 1H, Ar-NH) ppm. MS (ESI) m/z = 481.3 ($[\text{M}-\text{H}]^-$).

4-(2-(3,4-Dichloro-5-methyl-1*H*-pyrrole-2-carboxamido)-4-(3-ethylureido)phenoxy)piperidin-1-ium chloride (74a). Synthesized according to General procedure G from **73b** (55 mg, 0.099 mmol). Product was filtered off from the reaction mixture and washed with 20 mL of dichloromethane to give pure product as beige solid. Yield 70% (13 mg). ^1H NMR (400 MHz, DMSO) δ = 1.04 (t, 3H, J = 7.2 Hz, CH_2CH_3), 1.76 – 1.94 (m, 2H, piperidine- CH_2), 2.11 – 2.21 (m, 2H, piperidine- CH_2), 2.24 (s, 3H, pyrrole- CH_3), 2.95 – 3.17 (m, 4H, piperidine- CH_2 and CH_2CH_3), 3.22 – 3.34 (m, 2H, piperidine- CH_2), 4.64 (tt, 1H, J = 8.6, 3.8 Hz, piperidine-CH), 6.10 (t, 1H, J = 5.6 Hz, NHCH_2CH_3), 7.05 (d, 1H, J = 9.0 Hz, Ar-H-6), 7.29 (dd, 1H, J = 8.9, 2.6 Hz, Ar-H-5), 8.25 (d, 1H, J = 2.6 Hz, Ar-H-3), 8.52 (s, 1H, Ar-NH), 8.72 (bs, 1H, piperidine- NH_2 -A), 8.97 (bs and s overlapped, 2H, piperidine- NH_2 -B and Ar-NH), 12.37 (s, 1H, pyrrole-NH) ppm. ^{13}C NMR (100 MHz, DMSO- d_6) δ = 10.7, 15.5, 27.7, 33.9, 41.1, 71.0, 108.4, 109.5, 110.2, 113.2, 113.5, 118.9, 128.1, 129.2, 134.4, 139.6, 155.3, 156.1 ppm. HRMS for $\text{C}_{20}\text{H}_{26}\text{Cl}_2\text{N}_5\text{O}_3$ ($[\text{M}+\text{H}]^+$): calculated 454.1407, found 454.1399. HPLC purity 98.8%.

4-(2-Acetamido-4-(3-ethylureido)phenoxy)piperidin-1-ium chloride (74b). Synthesized according to General procedure G from **73c** (22 mg, 0.053 mmol). The reaction mixture was stirred overnight at reflux. Product was filtered off from the reaction mixture as brown solid. Yield 86% (42 mg). ^1H NMR (400 MHz, DMSO) δ = 1.03 (t, 3H, J = 7.2 Hz, CH_2CH_3), 1.81 – 1.96 (m, 2H, piperidine- CH_2), 1.98 – 2.06 (m, 2H, piperidine- CH_2), 2.09 (s, 3H, COCH_3), 2.98 – 3.14 (m, 4H, piperidine- CH_2 and CH_2CH_3), 3.21 – 3.34 (m, 2H, piperidine- CH_2), 4.50 (dt, 1H, J = 6.7, 3.4 Hz piperidine-CH), 6.04 (t, 1H, J = 5.6 Hz, NHCH_2CH_3), 6.95 (d, 1H, J = 8.9 Hz, Ar-H-6), 7.24 (dd, 1H, J = 8.9, 2.7 Hz, Ar-H-5), 7.73 (d, 1H, J = 2.7 Hz,

Ar-H-3), 8.44 (s, 1H, Ar-NH), 8.82 (bs, 2H, piperidine-NH₂), 9.09 (s, 1H, Ar-NH) ppm. ¹³C NMR (100 MHz, DMSO-*d*₆) δ = 15.9, 21.6, 26.9, 27.3, 34.3, 69.5, 114.3, 114.6, 118.0, 121.6, 134.9, 144.0, 155.8, 172.5 ppm. HRMS for C₁₆H₂₅N₄O₃ ([M+H]⁺): calculated 321.1921, found 321.1915. HPLC purity 95.5%.

4-(2-Benzamido-4-(3-ethylureido)phenoxy)piperidin-1-ium chloride (74c).

Synthesized according to General procedure G from **73d** (28 mg, 0.058 mmol). Product was filtered off from the reaction mixture as light yellow solid. Yield 33% (8 mg). ¹H NMR (400 MHz, DMSO) δ = 1.05 (t, 3H, *J* = 7.1 Hz, CH₂CH₃), 1.81 – 1.98 (m, 2H, piperidine-CH₂), 1.96 – 2.11 (m, 2H, piperidine-CH₂), 2.99 – 3.15 (m, 4H, piperidine-CH₂ and CH₂CH₃), 3.17 – 3.29 (m, 2H, piperidine-CH₂), 4.52 – 4.64 (m, 1H, piperidine-CH), 6.08 (t, 1H, *J* = 5.6 Hz, NHCH₂CH₃), 7.02 (d, 1H *J* = 9.0 Hz, Ar-H), 7.27 (dd, 1H, *J* = 8.9, 2.6 Hz, Ar-H), 7.50 – 7.58 (m, 2H, 2 × Ar-H) 7.58 – 7.66 (m, 1H, Ar-H), 7.73 (d, 1H, *J* = 2.6 Hz, Ar-H), 7.85 – 8.01 (m, 2H, 2 × Ar-H), 8.47 (s, 1H, Ar-NH), 8.66 (bs, 2H, piperidine-NH₂), 9.57 (s, 1H, Ar-NH) ppm. ¹³C NMR (100 MHz, DMSO-*d*₆) δ = 15.5, 27.0, 33.9, 69.5, 114.7, 115.5, 115.7, 127.4, 128.6, 131.6, 134.2, 134.6, 143.9, 155.3, 165.2 ppm. HRMS for C₂₁H₂₇N₄O₃ ([M+H]⁺): calculated 383.2078, found 383.2069. HPLC purity 97.7%.

Methyl 2-hydroxy-4-nitrobenzoate (76) [29]. Synthesized according to General procedure D from **75** (1.10 g, 6.01 mmol). Compound **76** was obtained as yellow solid. Yield 93% (1.10 g). ¹H NMR (400 MHz, DMSO) δ = 3.90 (s, 3H, COOCH₃), 7.72 (dd, 1H, *J* = 8.6, 2.3 Hz, Ar-H-5), 7.75 (dd, 1H, *J* = 2.3, 0.4 Hz, Ar-H-3), 7.93 (dd, 1H, *J* = 8.6, 0.5 Hz, Ar-H-6), 10.99 (s, 1H, Ar-OH) ppm.

Methyl 2-isopropoxy-4-nitrobenzoate (77) [29]. Synthesized according to General procedure A from **76** (700 mg, 3.55 mmol) and isopropanol (0.55 mL, 7.10 mmol). The crude product was purified with flash column chromatography using hexane/ethyl acetate (6/1) as an eluent to give **77** as yellow oil. Yield 80% (683 mg). ¹H NMR (400 MHz, CDCl₃) δ = 1.44 (d, 6H, *J* = 6.1 Hz, CH(CH₃)₂), 3.94 (s, 3H, COOCH₃), 4.73 (hept, *J* = 6.1 Hz, CH(CH₃)₂), 7.79 – 7.83 (m, 2H, 2 × Ar-H), 7.86 (d, 1H, *J* = 9.0 Hz, Ar-H-6) ppm.

2-Isopropoxy-4-nitrobenzamide (78). Synthesized according to General procedure E from **77** (250 mg, 1.05 mmol). Pure product was obtained after removing methanol under reduced pressure as light yellow crystals. Yield 96% (225 mg). ¹H NMR (400 MHz, DMSO) δ = 1.36 (d, 6H, *J* = 6.0 Hz, CH(CH₃)₂), 4.91 (hept, 1H, *J* = 5.9 Hz, CH(CH₃)₂), 7.69 (bs, 1H,

CONH₂-A), 7.80 (bs, 1H, CONH₂-B), 7.82 – 7.85 (dd, 1H, $J = 8.3, 2.1$ Hz, Ar-H-6), 7.86 – 7.89 (m, 2H, $2 \times$ Ar-H) ppm. MS (ESI) $m/z = 246.9$ ($[M+Na+H]^+$).

4-Amino-2-isopropoxybenzamide (79). Synthesized according to General procedure B from **78** (195 mg, 0.87 mmol). After removal of the solvent under reduced pressure, product was obtained as brown oil. Yield 97% (164 mg). ¹H NMR (400 MHz, CDCl₃) $\delta = 1.44$ (d, 6H, $J = 6.1$ Hz, CH(CH₃)₂), 4.01 (bs, 2H, Ar-NH₂), 4.69 (hept, 1H, $J = 6.1$ Hz, CH(CH₃)₂), 5.62 (bs, 1H, CONH₂-A), 6.22 (d, 1H, $J = 2.1$ Hz, Ar-H-3), 6.35 (dd, 1H, $J = 8.5, 2.1$ Hz, Ar-H-5), 7.79 (bs, 1H, CONH₂-B), 8.04 (d, 1H, $J = 8.5$ Hz, Ar-H-6) ppm. ¹³C NMR (100 MHz, CDCl₃) $\delta = 22.2, 71.6, 99.3, 107.7, 112.0, 134.3, 151.3, 157.9, 167.5$ ppm. MS (ESI) $m/z = 194.9$ ($[M+H]^+$)

N-(4-carbamoyl-3-isopropoxyphenyl)-3,4-dichloro-5-methyl-1H-pyrrole-2-carboxamide (80). Synthesized according to General procedure C from **79** (80 mg, 0.41 mmol). The product was suspended in dichloromethane/methanol (12/1) and filtered off from the reaction mixture as light brown solid. Yield 42% (63 mg). ¹H NMR (400 MHz, DMSO) $\delta = 1.39$ (d, 6H, $J = 6.0$ Hz, CH(CH₃)₂), 2.24 (s, 3H, pyrrole,CH₃), 4.70 (hept, 1H, $J = 6.0$ Hz, CH(CH₃)₂), 7.28 (dd, 1H, $J = 8.6, 1.9$ Hz, Ar-H-6), 7.51 (s, 2H, CONH₂), 7.63 (d, 1H, $J = 1.8$ Hz, Ar-H-2), 7.88 (d, 1H, $J = 8.6$ Hz, Ar-H-5), 9.65 (s, 1H, Ar-NHCO), 12.24 (s, 1H, pyrrole-NH) ppm. ¹³C NMR (100 MHz, DMSO-*d*₆) $\delta = 10.8, 21.7, 71.4, 105.0, 108.6, 111.6, 111.7, 117.6, 119.4, 128.4, 131.9, 142.5, 156.0, 157.4, 165.6$ ppm. HRMS for C₁₆H₁₈Cl₂N₃O₃ ($[M+H]^+$): calculated 370.0720, found 370.0716. HPLC purity 97.1%.

4.3. Determination of inhibitory activities against human DNA topoisomerase II α

Inhibitory activities against topo II α were determined with commercially available relaxation assay kits (Inspiralis Limited, Norwich, UK) on Pierce™ streptavidin coated 96-well microtiter plates (Thermo Scientific, Rockford, IL, USA). The plates were rehydrated with wash buffer (20 mM Tris·HCl, 137 mM NaCl, 0.01 % w/v BSA, 0.05 % v/v Tween 20, pH 7.6) and then biotinylated triplex forming oligonucleotide dissolved in wash buffer added for 5 minutes to immobilize. The unbound oligonucleotide was washed off with wash buffer. Next, enzymatic reaction was performed: the reaction volume of 30 μ L in buffer (50 mM Tris·HCl, 10 mM MgCl₂, 125 mM NaCl, 5 mM DTT, 0.1 μ g/mL albumin, 1 mM ATP, pH 7.5) contained 0.75 μ g of supercoiled pNO1 plasmid, 1.5 U of human DNA topoisomerase II, inhibitor, 1 % DMSO and 0.008 % Tween 20. Reaction mixtures were incubated at 37°C for 30 min. After that, the TF buffer (50 mM NaOAc, 50 mM NaCl and 50 mM MgCl₂, pH 5.0) was added and

the mixtures were left for 30 min at RT, during which biotin–oligonucleotide–plasmid triplex was formed. The unbound plasmid was washed off with TF buffer. Then the solution of Diamond Dye in T10 buffer (10 mM Tris·HCl, 1 mM EDTA, pH 8.0) was added. After 15 minutes of incubation in the dark, fluorescence was measured with a microplate reader (BioTek Synergy H4, excitation: 485 nm, emission: 537 nm). Initial screening was done at 10 and 100 μ M concentrations of inhibitors followed by IC₅₀ determination for active compounds, using seven concentrations of tested compounds. GraphPad Prism 6 software was used to calculate the IC₅₀ values. The results are reported as the average value of at least two independent measurements. As the positive control, etoposide (TCI, Tokyo, Japan; IC₅₀ = 71 μ M) was used.

4.4. Determination of inhibitory activities against bacterial DNA topoisomerases

Inhibitory activities against *E. coli* and *S. aureus* DNA gyrase and DNA topoisomerase IV were determined according to the protocol described in the reference [34].

4.5. Determination of mode of inhibition of compound **52** in DNA topoisomerase II α ATPase assay

To confirm the proposed ATP-competitive mode of inhibition of compound **52**, a linked assay (Inspiralis Ltd, Norwich, UK) was performed in which the hydrolysis of ATP is coupled to the oxidation of NADH through pyruvate kinase/lactate dehydrogenase system. The conversion of NADH to NAD⁺ was monitored with absorbance readings at 340 nm. To each well, 39.1 μ L of the following mix was added: assay buffer (5 μ L; 200 mM Tris-HCl, 1250 mM potassium acetate, 50 mM magnesium acetate, and 20 mM DTT [pH 7.9]), linear pBR322 (1.5 μ L, 1 mg/mL), phosphoenol pyruvate (0.5 μ L, 80 mM), pyruvate kinase/lactate dehydrogenase mix (0.75 μ L), NADH (1 μ L; 20 mM) and water (32.35 μ L). Then 2.5 μ L of the appropriate compound (diluted in DMSO) and 5 μ L of 140 nM topo II α were added. The change in absorbance was then measured in a plate reader for 10-15 minutes (prerun). 3.4 μ L of ATP solution in appropriate concentration was then added to start the run and the absorbance was monitored for 30 minutes at 37 °C.

From the data of absorbance measurements with time, the rates (absorbance change per minute) were calculated and then converted into the rates of ATP hydrolysis using an extinction coefficient of 6.22 M⁻¹cm⁻¹ and path length of 0.5 cm. For IC₅₀ determinations plots were made of percentage of ATPase activity against concentration of **52**. To determine the effect of ATP concentration on inhibition of topo II α ATPase activity, the rates of ATP hydrolysis were

plotted against ATP concentration for different **52** concentrations. SigmaPlot software was used for curve fittings.

First, IC₅₀ value of **52** at 2 mM ATP was determined, using nine concentration points between 0.05 μM and 50 μM. Based on that, concentrations of **52** for further assays were selected (0.1, 0.25, 0.5, 1 and 2.5 μM). At each inhibitor concentration an assay was performed at the following ATP concentrations: 0.05, 0.075, 0.1, 0.25, 0.5, 0.75, 1, 1.5 and 2 mM. All assays were performed in two independent experiments.

4.6. Determination of cytotoxic activities on MCF-7 and HepG2 cancer cell lines (MTS assay)

Cytotoxicity of compounds in HepG2 and MCF-7 cell lines was determined with MTS (3-(4,5-dimethylthiazol-2-yl)-5-(3-carboxymethoxyphenyl)-2-(4-sulfophenyl)-2H-tetrazolium) (Promega, Madison, WI, USA) assay according to manufacturer instructions. Briefly, HepG2 and MCF-7 cells were cultured in Eagle's MEM medium (Gibco, Thermo Fisher Scientific, Waltham, MA, USA) supplemented with 2 mM l-glutamine (Sigma-Aldrich, St. Louis, MO, USA), 100 U/mL penicillin (Sigma-Aldrich, St. Louis, MO, USA), and 100 μg/mL streptomycin (Sigma-Aldrich, St. Louis, MO, USA), and 10% FBS (Gibco, Thermo Fisher Scientific, Waltham, MA, USA) at 37 °C and under 5% CO₂. The cells were seeded in 96-well plates at a density of 2,000 cells per well, and allowed to attach overnight. After 24 h cells were treated with selected compounds, vehicle control (0.5% DMSO) or positive control (50 μM etoposide) and incubated for 72 h. 10 μL of CellTiter96[®] Aqueous One Solution Reagent (Promega, Madison, WI, USA) was then added to each well of the plate and incubated for another 3 h. Absorbance (490 nm) was measured with the automatic microplate reader Synergy[™] 4 Hybrid Microplate Reader (BioTek, Winooski, VT, USA). Independent experiments were run in triplicate and repeated three times. Statistical significance ($p < 0.05$) was calculated with two-tailed Welch's t test between treated groups and DMSO. IC₅₀ values that represent the concentration of the compound that gives a half-maximal response were determined using GraphPad Prism software (5.0) and are given as average values from the independent measurements. As the positive control, etoposide (TCI, Tokyo, Japan; MCF-7 IC₅₀ = 25 μM; HepG2 IC₅₀ = 20 μM) was used.

4.7. Molecular modelling

4.7.1 Alignment of binding sites

Both proteins were obtained from Protein Data Bank (ATPase domain of *E. coli* DNA gyrase; PDB: 4PRV, and ATPase domain of topo II α with AMP-PNP; PDB: 1ZXM) and prepared with Protein Preparation Wizard (default settings). Binding Site Alignment module from Schrödinger Release 2016-2 (New York, NY, USA, 2016) was used to align the binding sites. Visually results were presented as overlay of binding pose of ADP in the ATP binding site of *E. coli* DNA gyrase and binding pose of AMP-PNP in the ATP binding site of topo II α .

4.7.1 Molecular docking

Molecular docking study was performed using Schrödinger Suite, Release 2016-2 (Schrödinger, LLC, New York, NY, USA, 2016), with Maestro 11. First, a virtual library of compounds, that consisted of initial hits and designed compounds, was built in ChemDraw Professional 16.0 (PerkinElmer Inc., Massachusetts, USA). Then ligands were prepared with LigPrep module where OPLS 2005 force field was used for minimization and Epik to assign the correct protonation state. Protein was obtained from the Protein Data Bank (ATPase domain of topo II α with AMP-PNP; PDB: 1ZXM) and prepared with Protein Preparation Wizard (default settings). Receptor Grid Generation Panel was used to define the active site and hydrogen bond with Asn120 was set up as a constrain for docking. Glide XP docking module was used to perform the molecular docking. Docking protocol was validated by re-docking AMP-PNP in the binding site (RMSD = 0.755).

ASSOCIATED CONTENT

Appendix A: Supplementary information

Includes structures of compounds from initial screening, representative enzyme inhibition graphs, representative cell viability graphs and representative ^1H and ^{13}C NMR spectra of final compounds.

Acknowledgements

The authors thank Davide Benedetto Tiz, Helena Macut, Francesca Magari, Denise Lovison and Nataša Šijanec for synthesis of initial hits that were discussed in this manuscript (and many others whose compounds were also tested but turned out to be inactive), Sara Tratnik, Tjaša Debelak and Tjaša Permanšek for help with the cell-based assays. Dr. Nicolas Burton and Dr. Alison Howells from Inspiralis, Norwich, UK are acknowledged for performing human DNA topoisomerase II α ATPase assays.

Funding sources

This work was supported by the Slovenian Research Agency (Grant P1-0208).

REFERENCES

- [1] C. Bailly, Contemporary challenges in the design of topoisomerase II inhibitors for cancer chemotherapy, *Chem. Rev.* 112 (2012) 3611–3640. <https://doi.org/10.1021/cr200325f>.
- [2] J.J. Champoux, DNA topoisomerases: structure, function, and mechanism, *Annu. Rev. Biochem.* 70 (2001) 369–413. <https://doi.org/10.1146/annurev.biochem.70.1.369>.
- [3] J.E. Deweese, N. Osheroff, The use of divalent metal ions by type II topoisomerases, *Met. Integr. Biometal Sci.* 2 (2010) 450–459. <https://doi.org/10.1039/c003759a>.
- [4] R. Dutta, M. Inouye, GHKL, an emergent ATPase/kinase superfamily, *Trends Biochem. Sci.* 25 (2000) 24–28. [https://doi.org/10.1016/S0968-0004\(99\)01503-0](https://doi.org/10.1016/S0968-0004(99)01503-0).
- [5] N. Zidar, H. Macut, T. Tomašič, L. Peterlin Mašič, J. Ilaš, A. Zega, P. Tammela, D. Kikelj, New N-phenyl-4,5-dibromopyrrolamides as DNA gyrase B inhibitors, *MedChemComm.* 10 (2019) 1007–1017. <https://doi.org/10.1039/c9md00224c>.
- [6] D. Lafitte, V. Lamour, P.O. Tsvetkov, A.A. Makarov, M. Klich, P. Deprez, D. Moras, C. Briand, R. Gilli, DNA gyrase interaction with coumarin-based inhibitors: the role of the hydroxybenzoate isopentenyl moiety and the 5'-methyl group of the noviose, *Biochemistry.* 41 (2002) 7217–7223. <https://doi.org/10.1021/bi0159837>.
- [7] S. Narramore, C.E.M. Stevenson, A. Maxwell, D.M. Lawson, C.W.G. Fishwick, New insights into the binding mode of pyridine-3-carboxamide inhibitors of E. coli DNA gyrase, *Bioorg. Med. Chem.* 27 (2019) 3546–3550. <https://doi.org/10.1016/j.bmc.2019.06.015>.
- [8] P. Panchaud, T. Bruyère, A.-C. Blumstein, D. Bur, A. Chambovey, E.A. Ertel, M. Gude, C. Hubschwerlen, L. Jacob, T. Kimmerlin, T. Pfeifer, L. Prade, P. Seiler, D. Ritz, G. Rueedi, Discovery and Optimization of Isoquinoline Ethyl Ureas as Antibacterial Agents, *J. Med. Chem.* 60 (2017) 3755–3775. <https://doi.org/10.1021/acs.jmedchem.6b01834>.
- [9] M. Brvar, A. Perdih, M. Renko, G. Anderluh, D. Turk, T. Solmajer, Structure-based discovery of substituted 4,5'-bithiazoles as novel DNA gyrase inhibitors, *J. Med. Chem.* 55 (2012) 6413–6426. <https://doi.org/10.1021/jm300395d>.
- [10] S.M. Ronkin, M. Badia, S. Bellon, A.-L. Grillot, C.H. Gross, T.H. Grossman, N. Mani, J.D. Parsons, D. Stamos, M. Trudeau, Y. Wei, P.S. Charifson, Discovery of pyrazolthiazoles as novel and potent inhibitors of bacterial gyrase, *Bioorg. Med. Chem. Lett.* 20 (2010) 2828–2831. <https://doi.org/10.1016/j.bmcl.2010.03.052>.

- [11] A. Vanden Broeck, C. Lotz, J. Ortiz, V. Lamour, Cryo-EM structure of the complete E. coli DNA gyrase nucleoprotein complex, *Nat. Commun.* 10 (2019) 4935. <https://doi.org/10.1038/s41467-019-12914-y>.
- [12] H. Wei, A.J. Ruthenburg, S.K. Bechis, G.L. Verdine, Nucleotide-dependent domain movement in the ATPase domain of a human type IIA DNA topoisomerase. *J Biol Chem.* 280 (2005) 37041-7. <https://doi.org/10.1074/jbc.M506520200>
- [13] J.L. Nitiss, DNA topoisomerase II and its growing repertoire of biological functions, *Nat. Rev. Cancer.* 9 (2009) 327–337. <https://doi.org/10.1038/nrc2608>.
- [14] K. Morotomi-Yano, S. Saito, N. Adachi, K.-I. Yano, Dynamic behavior of DNA topoisomerase II β in response to DNA double-strand breaks, *Sci. Rep.* 8 (2018) 10344. <https://doi.org/10.1038/s41598-018-28690-6>.
- [15] V.K. Tiwari, L. Burger, V. Nikolettou, R. Deogracias, S. Thakurela, C. Wirbelauer, J. Kaut, R. Terranova, L. Hoerner, C. Mielke, F. Boege, R. Murr, A.H.F.M. Peters, Y.-A. Barde, D. Schübeler, Target genes of Topoisomerase II β regulate neuronal survival and are defined by their chromatin state, *Proc. Natl. Acad. Sci. U. S. A.* 109 (2012) E934-943. <https://doi.org/10.1073/pnas.1119798109>.
- [16] J.M. Berger, S.J. Gamblin, S.C. Harrison, J.C. Wang, Structure and mechanism of DNA topoisomerase II, *Nature.* 379 (1996) 225–232. <https://doi.org/10.1038/379225a0>.
- [17] B. Pogorelčnik, A. Perdih, T. Solmajer, Recent developments of DNA poisons--human DNA topoisomerase II α inhibitors--as anticancer agents, *Curr. Pharm. Des.* 19 (2013) 2474–2488. <https://doi.org/10.2174/1381612811319130016>.
- [18] C.W. Lindsley, S.F. Barnett, M. Yaroschak, M.T. Bilodeau, M.E. Layton, Recent progress in the development of ATP-competitive and allosteric Akt kinase inhibitors, *Curr. Top. Med. Chem.* 7 (2007) 1349–1363. <https://doi.org/10.2174/156802607781696864>.
- [19] C.J. Sherr, D. Beach, G.I. Shapiro, Targeting CDK4 and CDK6: From Discovery to Therapy, *Cancer Discov.* 6 (2016) 353–367. <https://doi.org/10.1158/2159-8290.CD-15-0894>.
- [20] A.D. Zuehlke, M.A. Moses, L. Neckers, Heat shock protein 90: its inhibition and function, *Philos. Trans. R. Soc. Lond. B. Biol. Sci.* 373 (2018). <https://doi.org/10.1098/rstb.2016.0527>.
- [21] P. Chène, J. Rudloff, J. Schoepfer, P. Furet, P. Meier, Z. Qian, J.-M. Schlaeppli, R. Schmitz, T. Radimerski, Catalytic inhibition of topoisomerase II by a novel rationally designed ATP-competitive purine analogue, *BMC Chem. Biol.* 9 (2009) 1. <https://doi.org/10.1186/1472-6769-9-1>.

- [22] P. Daumar, B.M. Zeglis, N. Ramos, V. Divilov, K.K. Sevak, N. Pillarsetty, J.S. Lewis, Synthesis and evaluation of ^{18}F -labeled ATP competitive inhibitors of topoisomerase II as probes for imaging topoisomerase II expression, *Eur. J. Med. Chem.* 86 (2014) 769–781. <https://doi.org/10.1016/j.ejmech.2014.09.019>.
- [23] H. Huang, Q. Chen, X. Ku, L. Meng, L. Lin, X. Wang, C. Zhu, Y. Wang, Z. Chen, M. Li, H. Jiang, K. Chen, J. Ding, H. Liu, A series of alpha-heterocyclic carboxaldehyde thiosemicarbazones inhibit topoisomerase II α catalytic activity, *J. Med. Chem.* 53 (2010) 3048–3064. <https://doi.org/10.1021/jm9014394>.
- [24] A.T. Baviskar, C. Madaan, R. Preet, P. Mohapatra, V. Jain, A. Agarwal, S.K. Guchhait, C.N. Kundu, U.C. Banerjee, P.V. Bharatam, N-Fused Imidazoles As Novel Anticancer Agents That Inhibit Catalytic Activity of Topoisomerase II α and Induce Apoptosis in G1/S Phase, *J. Med. Chem.* 54 (2011) 5013–5030. <https://doi.org/10.1021/jm200235u>.
- [25] V. Furlanetto, G. Zagotto, R. Pasquale, S. Moro, B. Gatto, Ellagic acid and polyhydroxylated urolithins are potent catalytic inhibitors of human topoisomerase II: an in vitro study, *J. Agric. Food Chem.* 60 (2012) 9162–9170. <https://doi.org/10.1021/jf302600q>.
- [26] K. Y. Jun, E.Y. Lee, M.J. Jung, O.H. Lee, E.S. Lee, H.Y. Park Choo, Y. Na, Y. Kwon, Synthesis, biological evaluation, and molecular docking study of 3-(3'-heteroatom substituted-2'-hydroxy-1'-propyloxy) xanthone analogues as novel topoisomerase II α catalytic inhibitor, *Eur. J. Med. Chem.* 46 (2011) 1964–1971. <https://doi.org/10.1016/j.ejmech.2011.01.011>
- [27] K. Bergant, M. Janežič, K. Valjavec, I. Sosič, S. Pajk, M. Štampar, B. Žegura, S. Gobec, M. Filipič, A. Perdih, Structure-guided optimization of 4,6-substituted-1,3,5-triazin-2(1H)-ones as catalytic inhibitors of human DNA topoisomerase II α , *Eur. J. Med. Chem.* 175 (2019) 330–348. <https://doi.org/10.1016/j.ejmech.2019.04.055>.
- [28] N. Nakada, H. Gmünder, T. Hirata, M. Arisawa, Mechanism of inhibition of DNA gyrase by cyclothialidine, a novel DNA gyrase inhibitor, *Antimicrob. Agents Chemother.* 38 (1994) 1966–1973. <https://doi.org/10.1128/aac.38.9.1966>.
- [29] M. Durcik, D. Lovison, Ž. Skok, C. Durante Cruz, P. Tammela, T. Tomašič, D. Benedetto Tiz, G. Draskovits, Á. Nyerges, C. Pál, J. Ilaš, L. Peterlin Mašič, D. Kikelj, N. Zidar, New *N*-phenylpyrrolamide DNA gyrase B inhibitors: Optimization of efficacy and antibacterial activity, *Eur. J. Med. Chem.* 154 (2018) 117–132. <https://doi.org/10.1016/j.ejmech.2018.05.011>.

- [30] D.B. Tiz, Ž. Skok, M. Durcik, T. Tomašič, L.P. Mašič, J. Ilaš, A. Zega, G. Draskovits, T. Révész, Á. Nyerges, C. Pál, C.D. Cruz, P. Tammela, D. Žigon, D. Kikelj, N. Zidar, An optimised series of substituted *N*-phenylpyrrolamides as DNA gyrase B inhibitors, *Eur. J. Med. Chem.* 167 (2019) 269–290. <https://doi.org/10.1016/j.ejmech.2019.02.004>.
- [31] M. Gjorgjieva, T. Tomašič, M. Barančokova, S. Katsamakas, J. Ilaš, P. Tammela, L. Peterlin Mašič, D. Kikelj, Discovery of Benzothiazole Scaffold-Based DNA Gyrase B Inhibitors, *J. Med. Chem.* 59 (2016) 8941–8954. <https://doi.org/10.1021/acs.jmedchem.6b00864>.
- [32] M. Durcik, P. Tammela, M. Barancokova, T. Tomasic, J. Ilas, D. Kikelj, N. Zidar, Synthesis and Evaluation of *N*-Phenylpyrrolamides as DNA Gyrase B Inhibitors., *ChemMedChem.* 13 (2018) 186–198. <https://doi.org/10.1002/cmdc.201700549>.
- [33] T. Tomašič, S. Katsamakas, Ž. Hodnik, J. Ilaš, M. Brvar, T. Solmajer, S. Montalvão, P. Tammela, M. Banjanac, G. Ergović, M. Anderluh, L. Peterlin Mašič, D. Kikelj, Discovery of 4,5,6,7-Tetrahydrobenzo[1,2-*d*]thiazoles as Novel DNA Gyrase Inhibitors Targeting the ATP-Binding Site, *J. Med. Chem.* 58 (2015) 5501–5521. <https://doi.org/10.1021/acs.jmedchem.5b00489>.
- [34] N. Zidar, H. Macut, T. Tomašič, M. Brvar, S. Montalvão, P. Tammela, T. Solmajer, L. Peterlin Mašič, J. Ilaš, D. Kikelj, *N*-Phenyl-4,5-dibromopyrrolamides and *N*-Phenylindolamides as ATP Competitive DNA Gyrase B Inhibitors: Design, Synthesis, and Evaluation, *J. Med. Chem.* 58 (2015) 6179–6194. <https://doi.org/10.1021/acs.jmedchem.5b00775>.
- [35] N. Zidar, S. Montalvão, Ž. Hodnik, D.A. Nawrot, A. Žula, J. Ilaš, D. Kikelj, P. Tammela, L.P. Mašič, Antimicrobial activity of the marine alkaloids, clathrodin and oroidin, and their synthetic analogues, *Mar. Drugs.* 12 (2014) 940–963. <https://doi.org/10.3390/md12020940>.
- [36] J.W. Phillips, M.A. Goetz, S.K. Smith, D.L. Zink, J. Polishook, R. Onishi, S. Salowe, J. Wiltsie, J. Allocco, J. Sigmund, K. Dorso, S. Lee, S. Skwish, M. de la Cruz, J. Martín, F. Vicente, O. Genilloud, J. Lu, R.E. Painter, K. Young, K. Overbye, R.G.K. Donald, S.B. Singh, Discovery of kibdelymycin, a potent new class of bacterial type II topoisomerase inhibitor by chemical-genetic profiling in *Staphylococcus aureus*, *Chem. Biol.* 18 (2011) 955–965. <https://doi.org/10.1016/j.chembiol.2011.06.011>.
- [37] J. Lu, S. Patel, N. Sharma, S.M. Soisson, R. Kishii, M. Takei, Y. Fukuda, K.J. Lumb, S.B. Singh, Structures of kibdelymycin bound to *Staphylococcus aureus* GyrB and ParE

- showed a novel U-shaped binding mode, *ACS Chem. Biol.* 9 (2014) 2023–2031. <https://doi.org/10.1021/cb5001197>.
- [38] B. Fois, Ž. Skok, T. Tomašič, J. Ilaš, N. Zidar, A. Zega, L. Peterlin Mašič, P. Szili, G. Draskovits, Á. Nyerges, C. Pál, D. Kikelj, Dual *Escherichia coli* DNA Gyrase A and B Inhibitors with Antibacterial Activity, *ChemMedChem.* 15 (2020) 265–269. <https://doi.org/10.1002/cmdc.201900607>.
- [39] T. Tomašič, M. Mirt, M. Barančoková, J. Ilaš, N. Zidar, P. Tammela, D. Kikelj, Design, synthesis and biological evaluation of 4,5-dibromo-*N*-(thiazol-2-yl)-1*H*-pyrrole-2-carboxamide derivatives as novel DNA gyrase inhibitors, *Bioorg. Med. Chem.* 25 (2017) 338–349. <https://doi.org/10.1016/j.bmc.2016.10.038>.
- [40] L. Malca-Mor, A.A. Stark, Mutagenicity and toxicity of carcinogenic and other hydrazine derivatives: correlation between toxic potency in animals and toxic potency in *Salmonella typhimurium* TA1538., *Appl. Environ. Microbiol.* 44 (1982) 801–808.
- [41] P. Furet, J. Schoepfer, T. Radimerski, P. Chène, Discovery of a new class of catalytic topoisomerase II inhibitors targeting the ATP-binding site by structure based design. Part I, *Bioorg. Med. Chem. Lett.* 19 (2009) 4014–4017. <https://doi.org/10.1016/j.bmcl.2009.06.034>.
- [42] M.D. Shultz, Setting expectations in molecular optimizations: Strengths and limitations of commonly used composite parameters, *Bioorg. Med. Chem. Lett.* 23 (2013) 5980–5991. <https://doi.org/10.1016/j.bmcl.2013.08.029>.
- [43] N.R. Stokes, H.B. Thomaides-Brears, S. Barker, J.M. Bennett, J. Berry, I. Collins, L.G. Czaplewski, V. Gamble, P. Lancett, A. Logan, C.J. Lunniss, H. Peasley, S. Pommier, D. Price, C. Smee, D.J. Haydon, Biological Evaluation of Benzothiazole Ethyl Urea Inhibitors of Bacterial Type II Topoisomerases, *Antimicrob. Agents Chemother.* 57 (2013) 5977–5986. <https://doi.org/10.1128/AAC.00719-13>.
- [44] T. Tomašič, M. Barančoková, N. Zidar, J. Ilaš, P. Tammela, D. Kikelj, Design, synthesis, and biological evaluation of 1-ethyl-3-(thiazol-2-yl)urea derivatives as *Escherichia coli* DNA gyrase inhibitors, *Arch. Pharm. (Weinheim).* 351 (2018). <https://doi.org/10.1002/ardp.201700333>.
- [45] S. Bhadra, W.I. Dzik, L.J. Gooben, Synthesis of Aryl Ethers from Aromatic Carboxylic Acids, *Synthesis.* 45 (2013) 2387–2390. <https://doi.org/10.1055/s-0033-1339470>.
- [46] T. Gonec, I. Zadrazilova, E. Nevin, T. Kauerova, M. Pesko, J. Kos, M. Oravec, P. Kollar, A. Coffey, J. O'Mahony, A. Cizek, K. Kralova, J. Jampilek, Synthesis and Biological

- Evaluation of N-Alkoxyphenyl-3-hydroxynaphthalene-2-carboxanilides, *Molecules*. 20 (2015) 9767–9787. <https://doi.org/10.3390/molecules20069767>.
- [47] A.J. MacNair, M.-M. Tran, J.E. Nelson, G.U. Sloan, A. Ironmonger, S.P. Thomas, Iron-catalysed, general and operationally simple formal hydrogenation using Fe(OTf)₃ and NaBH₄, *Org. Biomol. Chem.* 12 (2014) 5082–5088. <https://doi.org/10.1039/c4ob00945b>.
- [48] Y.J. Zhu, F. Chen, Microwave-Assisted Preparation of Inorganic Nanostructures in Liquid Phase, *Chem. Rev.* 114 (2014) 6462–6555. <https://doi.org/10.1021/cr400366s>.
- [49] J. He, M. Wassar, K.S.L. Chan, Q. Shao, J.Q. Yu, Palladium-Catalyzed Transformations of Alkyl C–H Bonds, *Chem. Rev.* 117 (2017) 8754–8786. <https://pubs.acs.org/doi/10.1021/acs.chemrev.6b00622>.
- [50] R.L. Danheiser, R.F. Miller, R.G. Brisbois, S.Z. Park, An improved method for the synthesis of α -diazo ketones, *J. Org. Chem.* 55 (1990) 1959–1964. <https://doi.org/10.1021/jo00293a053>.

Highlights

- **Discovery of novel chemotype of DNA topoisomerase II inhibitors**
- **Bacterial topoisomerase inhibitors were an excellent starting point in search of new topo II inhibitors**
- **The most potent inhibitor had an IC_{50} of 3.2 μ M on topo II**
- **Two compounds showed very potent activity on MCF-7 cell line ($IC_{50} < 10 \mu$ M)**

Journal Pre-proofs